Technical Annex 7.2f - Deliverable Report on C.2 Action second year

Monitoring of SOC stabilization and the improvement of physical and biological soil fertility

Project responsible. CERMANU

List of abbreviations

AMF: arbuscular mychorrhyza fungi; **^{13}C/^{31}P-CPMAS NMR:** solid state Cross Polarization Magic Angle Spinning Nuclear Magnetic Resonance on ^{13}C; **FAME**: Fatty acids methyl ester; **HA**: Humic acids; **N/PLFA:** Neutral/Phospho-lipid fatty acids; **MWDw**: mean weight diameter in water; **N**: nitrogen; **S/TOC** soil/total organic carbon; **SOM:** Soil organic matter; **TAHMs-GC-MS**: off-line thermally assisted hydrolysis and methylation pyrolysis GasChromatography Mass Spectrometry

1. Codes of soil treatments according with Project sites

Piemonte: Tetto Frati,

Trad: traditional agronomic technique **0 N**: no Nitrogen fertilization; **SSB** and **SSA** low (1000 kg of C ha^{-1} and high (2000 kg of C ha^{-1}) dose of fresh solid phases of digestate; **CMPB** and **CMPA** low (1000 kg of C ha^{-1} and high (2000 kg of C ha^{-1}) dose of compost; **Fe-P** : traditional agronomic technique with addition of biomimetic catalyst (0.5g m^{-2}).

Grandi

Trad: traditional agronomic technique **0 N**: no Nitrogen fertilization; **SSB** and **SSA** low (1000 kg of C ha^{-1} and high (2000 kg of C ha^{-1}) dose of fresh solid phases of digestate; **CMPB** and **CMPA** low (1000 kg of C ha^{-1} and high (2000 kg of C ha^{-1}) dose of compost;

Campania

Castel Volturno

Trad: traditional agronomic technique **CMPB** and **CMPA** low (10 tons ha^{-1} and high (20 tons ha^{-1}) dose of on farm compost; **Fe-P** : traditional agronomic technique with addition of biomimetic catalyst (0.5g m^{-2}).

Prima Luce

A control no fertilization; **B** traditional organo-mineral fertilizer (Oligomax 8/5/10) 250 kg ha^{-1}; **C** LIFE on-farm compost 10 tons ha^{-1}; **D** LIFE on-farm compost 20 tons ha^{-1}

Mellone

Two systems: kiwi and peach; two composts: **A** “summer” and **B** “winter” depending on the crop residues used in composting process; three doses **0**-control , **1**- 10 tons ha-1, **2** - 20 tons ha-1

2. Materials and Methods

2.1 Soil aggregate stability

A modified procedure of the classical method described by Kemper and Rosenau (1986) was used to separate the water-stable aggregates. Forty grams of the <2.00 mm, air-dried soil samples were put in the topmost of a nest of three sieves of 1.00, 0.50 and 0.25mm mesh size and pre-soaked in distilled water for 30 min. Thereafter the nest of sieves and its contents were oscillated vertically in water 20 times using a 4 cm amplitude at the rate of one oscillation per second. Care was taken to ensure that the soil particles on the topmost sieve were always below the water surface during each oscillation. After wet-sieving, the resistant soil materials on each sieve and the unstable (<0.25 mm) aggregates were quantitatively transferred into beakers, dried in the oven at 50◦C for 48 h, weighed and stored.. The percentage ratio of the aggregates in each sieve represents the water-stable aggregates of size classes: 2.00–1.00, 1.00–0.50, 0.50–0.25 and <0.25 mm. Mean-weight diameter in water (MWDw) of water-stable aggregates was calculated as follow

$$MWDw = \sum_{i=1}^{n} Xi\ Wi$$

where Xi is the mean diameter of the *ith* sieve size and Wi the proportion of the total aggregates in the *ith* fraction.

2.2. Soil organic matter analyses

2.2 1Elemental analyses

TOC and total N in bulk soils and soil aggregates were determined by Fisons EA 1108 Elemental Analyzer (Fisons Instruments S.p.A., Rodana, MI, Italy). The soil samples were firstly dried in a oven at 40 °C and ground to a fine powder using a quartz agate mortar and pestle.

2.2.2 TAHM -GC-MS

Pyrolysis in the presence of tetramethyl ammonium hydroxide (TMAH) is commonly used to study the detailed molecular composition of either natural and synthetic biopolymers. It involves the cleavage of covalent bonds combined with the solvolysis and methylation of ester and ether groups, in complex mixture of organic macromolecules and biopolymers, thereby enhancing the thermal stability of acidic, alcoholic, and phenolic groups and allowing a suitable chromatographic detection of pyrolytic products.

For off line-THM-GC-MS about 2 g of soil samples were placed in a quartz boat with 2 mL of TMAH (25% in methanol w/v) solution. After drying under a stream of nitrogen, the mixture was introduced into a Pyrex tubular reactor (50 cm × 3.5 cm i.d.) and heated at 400 °C for 30 min in a circular oven (Barnstead Thermolyne 21100 Furnace, Barnstead International, Dubuque, IA, USA). The gaseous products from thermochemolysis were flowed into two chloroform (50 mL) traps in series, kept in ice/salt baths. The chloroform solutions were combined and rotoevaporated to dryness. The residue was dissolved in 1 mL of chloroform and transferred in a glass vial for GC-MS analysis. The GC-MS analyses were conducted with a Perkin Elmer Autosystem XL by using a RTX-5MS WCOT capillary column (Restek, 30 m × 0.25 mm; film thickness, 0.25 mm) that was coupled, through a heated transfer line (250 °C), to a PE Turbomass-Gold quadrupole mass spectrometer. The chromatographic separation was achieved with the following temperature program: 60 °C (1 min. isothermal), rate 7 °C min−1 to 320 °C (10 min. isothermal). Helium was used as carrier gas at 1.90 mL min−1, the injector temperature was at 250 °C, and the split-injection mode had a 30 mL min−1 of split flow. Mass spectra were obtained in EI mode (70 eV), scanning in the range 45–650 m/z, with a cycle time of 0.2 s. Compound identification was based on comparison of mass spectra with the NIST-library database, published spectra, and real standards.

For quantitative analysis, due to the large variety of detected compounds with different chromatographic responses, external calibration curves were built by mixing methyl esters and/or methyl ethers of the following molecular standards: tridecanoic acid, octadecanol, 16-hydroxyhexadecanoic acid, docosandioic acid, *â*-sitosterol, and cinnamic acid. Increasing amounts of standard mixtures were placed in a quartz boat and moistened with 0.5 mL of TMAH (25% in methanol) solution. The same thermochemolysis conditions as for compost samples were applied for the standards. The percentage recovery of standards ranged from 82 to 91% of initial amount.

2.2.3 13C isotopic analyses

The measurements will be performed on bulk samples provided by sampling procedure from each project site and on soil fractions deriving from the determination of soil aggregate stability. The analyses will be carried out in triplicates with continuous-flow isotope ratio mass spectrometry (IRMS) Results were expressed in the relative δ per mil scale, according to the equation:

$$\delta 13C\ ‰ = (Rsample/Rstandard\ -1) \times 1000$$

where R= 13C/12C, and the standard is referred to the international reference Pee Dee Belemnite (PDB). At initial and final sampling date, the amount of TOC derived compost addition in bulk soil and aggregate-size fractions is calculated as follows:

$$13C\text{-}OC = Ct \times (\delta s - \delta c)/(\delta 0 - \delta c)$$

where Ct indicates total C of sample, δ s is the δ13C value in the sample, δ0 is the δ 13C of the added compost and δc is the δ13C value of control sample.

2.2.4 Humic acids

The HA were extracted by the initial control soils following the classical procedure of the International Humic Science Society (IHSS). Briefly 50 g of soil were extracted with 400 ml of NaOH (0.1 M) and Na4P2O7*10H2O (0.01M) 1:8 extraction (soil:solution). Thereafter, the bottles were put in a horizontal shaker at 120 rpm for 24 hours. The solution was centrifuged at 7000 rpm for 20 minutes to separate better the solution from the soil fractions. Subsequently, the supernatant solution was filtered with glass fibres and it was acidified at pH 1 with HCL (12M) to promote the precipitation of HA, since they are insoluble at pH < 2. The acidified solution was allowed to stand on a bench overnight, then it was centrifuged at 7000 rpm for 20 minutes to recover the HA fraction. The HA were treated with HF and HCl to remove co-extracted inorganic impurities. The HA were dissolved in 100 ml of solution containing 2.5 ml of HCL (37%) and 2.5 ml of HF (40%) in 1L of deionised water and left for 24 hours in a horizontal shaker at 120 rpm. Thereafter, the solution was centrifuged at 7000 rpm for 20 min: the supernatant was discharged, while the HA precipitated was re-dissolved in deionised water and transferred into dialysis membranes (Spectrapore 3, 3500 Mw cut-off) and dialysed against deionised water until the dialysis water gives an electrical conductivity of 15 µS/cm. Once the dialysis was finished the sample were put in a freezer at -20 °C and subsequently freeze-dried.

The HA were characterized by 13C CPMAS NMR. Fine-powdered composite samples were analyzed by solid-state NMR spectroscopy (13C CPMAS NMR) on a Bruker AV300 Spectrometer equipped with a 4 mm wide-bore MAS probe. The NMR spectra were obtained by applying the following parameters: 13,000 Hz of rotor spin rate; 2 s of recycle time; 1H-power for CP 92.16 W: 1H 90° pulse 2.85 µs; 13C power for CP 150,4 W; 1 ms of contact time; 30 ms of acquisition time; 4000 scans. Samples were packed in 4 mm zirconium rotors with Kel-F caps. The cross polarization pulse sequence was applied with a composite shaped “ramp” pulse on the 1H channel in order to account for the inhomogeneity of Hartmann-Hann condition at high rotor spin frequency. The Fourier transform was performed with 4 k data point and an exponential apodization of 50 Hz of line broadening. The different carbon functionalities are conventionally grouped into the following chemical shift regions: alkyl-C: 0–45 ppm; methoxyl-C: 45–60 ppm; O-alkyl- C: 60–110 ppm; aryl-C: 110–145 ppm; phenol-C: 145– 160 ppm, and carboxyl-C: 190–160 ppm. The relative contribution of each region was determined by integra- tion (MestreNova 6.2.0 software, Mestre-lab Research, 2010), and expressed as percentage of the total area.

2.3 Biological analyses

2.3.1 PLFA

The neutral and phospholipid fatty acid (NLFA and PLFA) analysis are used to study microbial biomass and community structure of soil samples. This analytical method is based on the identification of fatty acids as biomarkers to determine the presence and abundance of broad functional microbial groups such as fungi, arbuscular mycorrhizal, gram positive (+) and negative (-) bacteria, actinomyces, etc. This method is often used to determine gross changes in the microbial community associated with different environmental conditions.

For the analysis, 50 gr of soil was collected from the rhizosphere of field plots The soil sampling was performed during crop cycle about 70 days after sowing. For the extraction of PLFA and NLFA 1 gram of dried soil was extracted for 2 hours with a mixture of chloroform/methanol/citrate buffer at pH 4 (1:2:0.8 v/v). After centrifugation, the upper phase was collected and split into two phases by adding chloroform and citrate buffer. The lower phase was recovered and dried with N flux. Thereafter, the lipids are fractionated into neutral, glycol- and phospho- lipids on a silica gel column by elution with chloroform, acetone and methanol, respectively. The neutral and phospholipids were dried under N2 flux at 37 °C and stored at -20 °C. Neutral and phospholipids were hydrolysed to free fatty acids by alkalization and consequently derivatized into fatty acids methyl esters. In this step methyl nonadecanoate fatty acid (19:0) was added to the sample as internal standard. The FAME are then separated from the head groups by using n-hexane and analysed by GC/MS. A PerkinElmer Autosystem XL (GC) equipped with a PE Turbomass-Gold quadrupole mass spectrometer was used.

The relative area of the chromatographic peak obtained for each PLFA and NLFA was divided by that of the internal standard (19:0). Each PLFA and NLFA content was expressed as nmol of PLFA per gram of wet soil. The concentration of PLFA were summed together to obtain the estimation of total biomass. In the case of arbuscular mycorrhiza (AM) fungi, C16:1ω5 NLFA were used as indicators of arbuscular mycorrhiza.(AM) fungi. In particular, this NLFA was taken into account as representative of spores and propagules of AM fungi, reflecting therefore the AM fungal growth. As marker of the AM fungi biomass the C16:1ω5 PLFA can be also considered. However, it is not entirely specific only for AMF, but it can also be representative of for some Gram- bacteria. To assess whether this PLFA indicates the presence of AM fungi or Gram- bacteria, the ratio between the NLFA and PLFA is calculated. If the NFLA/PLFA ratio is between 1 and 200 the PLFA is representing AM fungi, while if the ratio is lower than 1 it must be considered biomarkers of Gram- bacteria.

2.3.2 Enzimatic activity and ergosterol content

The ergosterol is a membrane lipid almost exclusive of fungi, homologous to cholesterol of animal cells. It represents a quite constant fraction of fungal hyphae (0.5-1.5 %) and is decomposed rapidly upon death of hypae. For this reasons, the ergosterol content is considered a good indicator of fungal biomass in soil. The utility of its measurement is related to the importance of fungi functions in soil ecosystem. The ergosterol in soil samples was extracted as follows: 2 g of fresh sieved (2 mm) soil in 10 ml test tubes were added with 4 ml of 10% KOH dissolved in methanol. The tubes were sonicated for 15 min and heated for 90 min at 70 °C. After cooling, 1 ml of ultrapure water and 2 ml of cyclohexane were added and the tubes were vortexed for 30 sec. The hydrophobic (cyclohexane) phase containing the sterols was separated from the hydrophilic phase by centrifuging for 5 min at 3000 rpm. The cycloexane (the upper) phase was collected by Pasteur

pipette and transferred to new test tubes. The cyclohexane was evaporated under a gentle N flow and the dried samples were dissolved in 1 ml of methanol. The ergosterol was measured by HPLC equipped with a C18 reverse-phase column and UV light detector at 282 nm. Methanol was used as mobile phase (1 ml min^{-1} flow rate).

3 Results

3.1 Soil aggregate stability

The differences in aggregate distribution and aggregate stability (MWDw found among project sites have to be mainly referred to the effects of textural composition. In fact the larger clay content in soil samples from Castel Volturno act as stabilizing agent, while the sandy soils from Piemonte show a lower aggregate stability, with the larger amount of soil fraction accumulating in the finest soil aggregates sizes (< 0.50 mm). The silty soil from Prima Luce is characterized by an intermediate behaviour (Figs 1, 2, 3, 4).

After two year of SOM management, distinct behaviours were found in the aggregate yields and stability index from the field treatments of different project sites, whose overall distribution were still affected by the large influence of different textural composition (Figs1, 2, 3, 4). At Tetto Frati (Fig. 1) the soil amendments with fresh solid digestate (SS-B and SS-A) and higher dose of composted material (CMPA), produced a decrease of unstable micro-aggregates (< 0.25 mm) which were incorporated in the intermediate macro-aggregate size fractions, with consequent increase of MWDw values. Similar trend was observed in the field plots of Grandi, where only the two soil treatments based on the addition of fresh solid digestate promoting an incorporation of finest soil fraction in the most stable macro-aggregates classes (Fig, 2) This effect may be associated with the availability of bio-available components which may favour the development of microbial biomass and related by-products that promote a transient binding action on soil aggregate.

The main influence of textural composition was shown in the soil distribution of field plots of Castel Volturno (Fig. 3), which did not reveal any valuable effect of soil treatment on aggregates and stability index.

Conversely a steady improvement of soil aggregation was found in soil samples amended with on farm compost at Prima Luce (Fig. 4). For both years the input of exogenous OM added with low and high dose of compost, produced an decrease of unstable microaggregate (< 0.25 mm), shifted into upper size fraction (1-0.50 mm), thereby revealing an average 30% increase in the stability index of soil sample with large compos addition (MWD 0.6 –D plots) in respect to conventional management (MWD 0.44 –A plots)

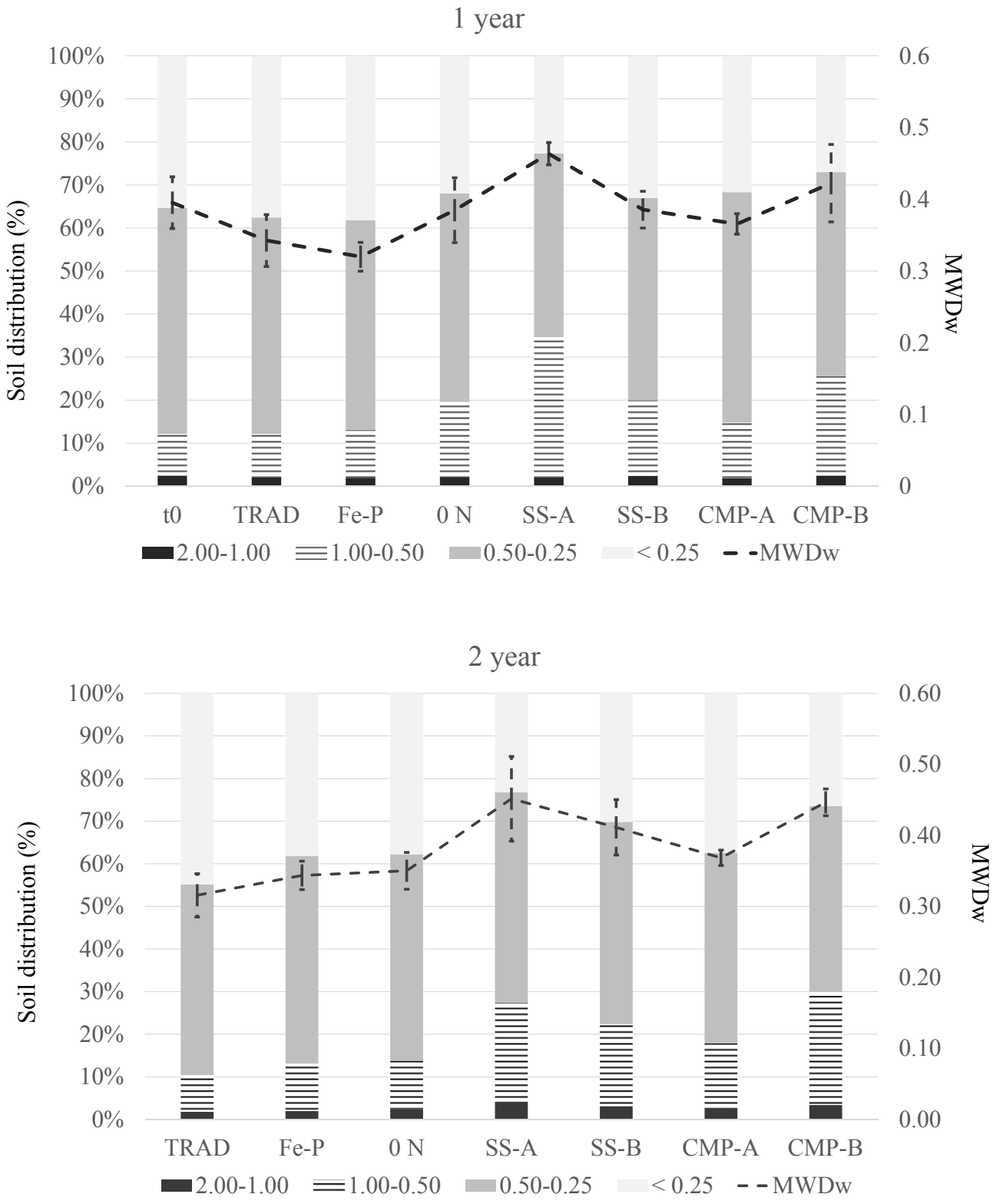

Figure 1. Tetto Frati: distribution (%) of water-stable aggregate sizes (mm) and stability index (MWD) in different field treatments

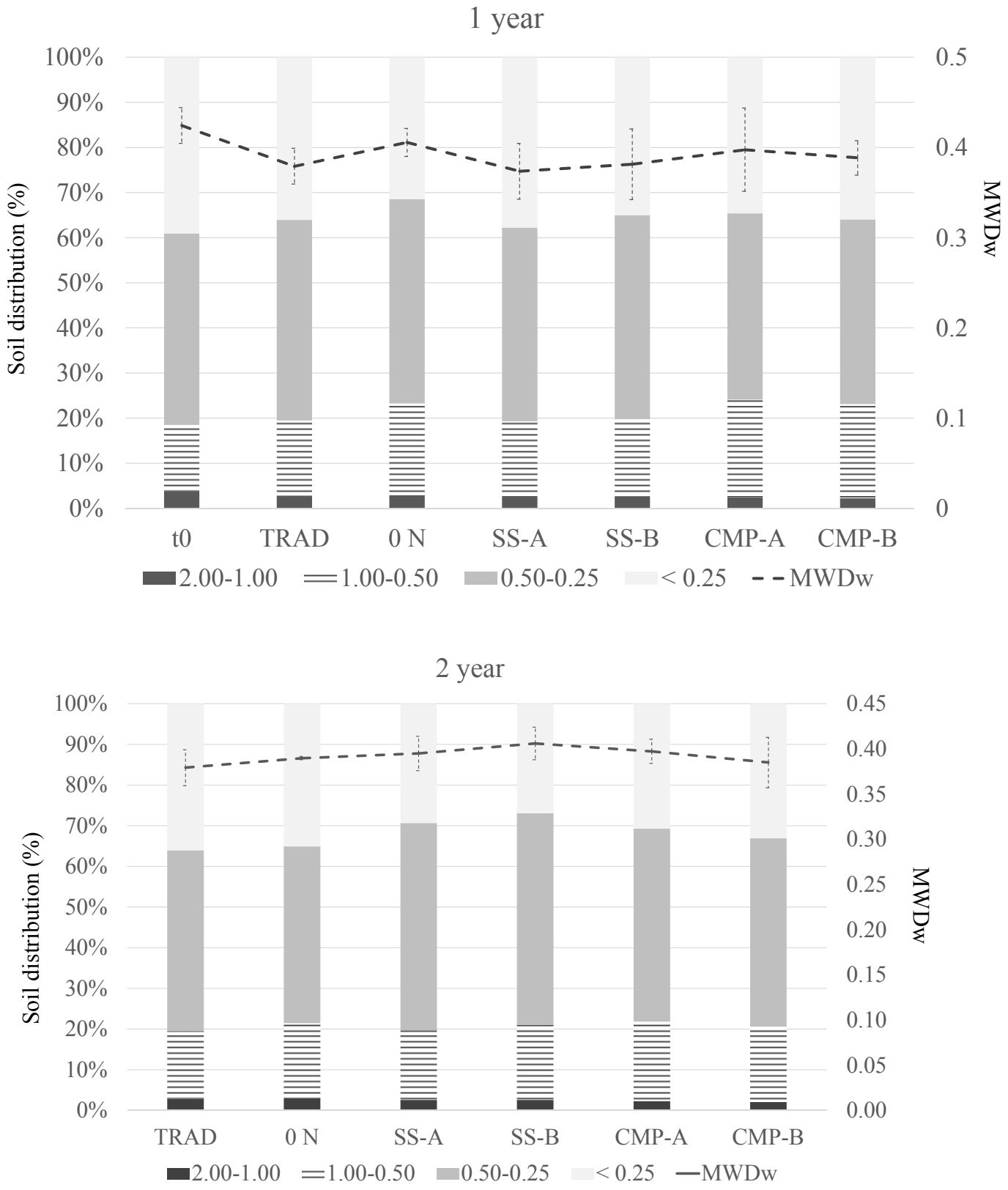

Figure 2. Grandi: distribution (%) of water-stable aggregate sizes (mm) and stability index (MWD) in different field treatments

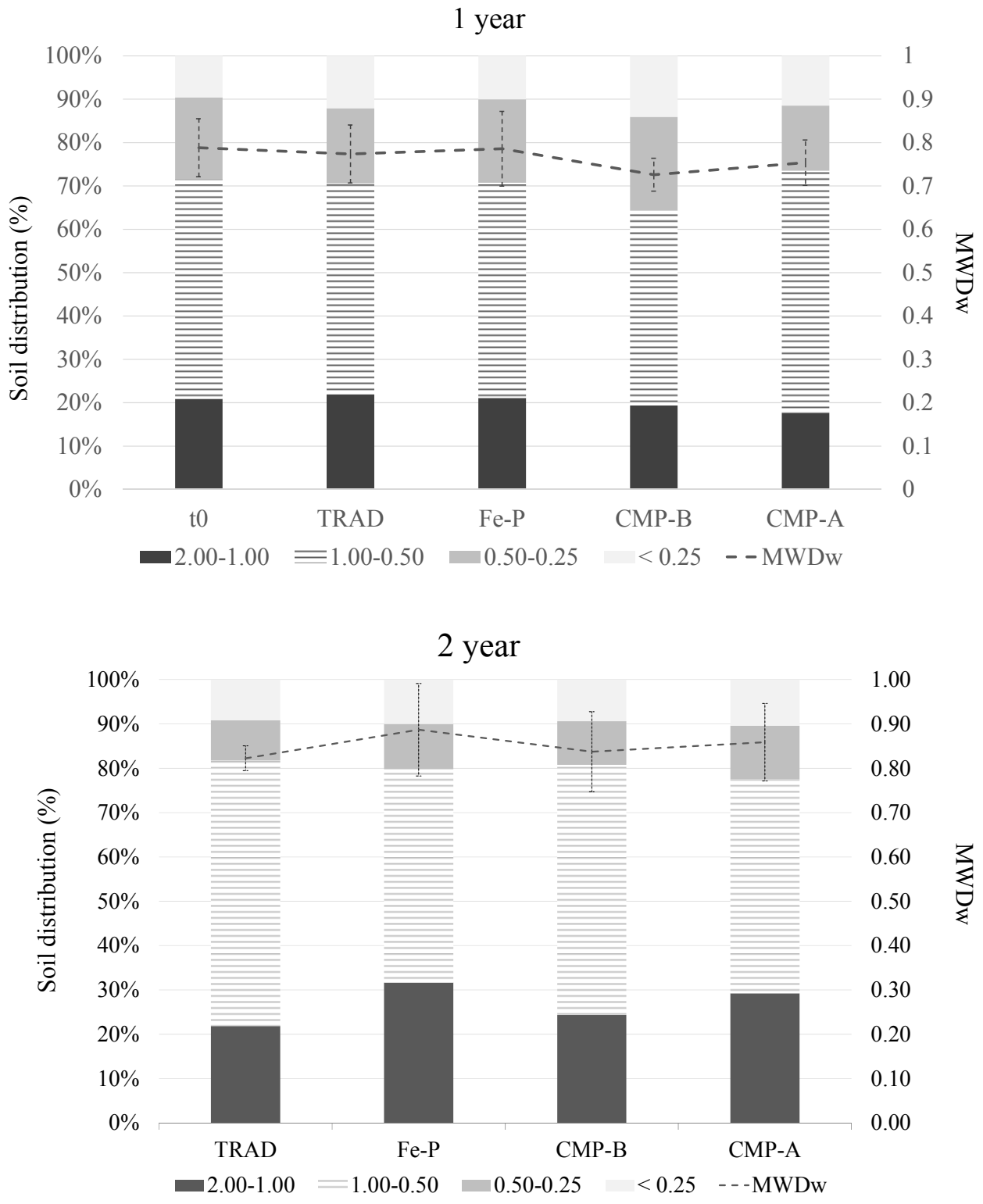

Figure 3 Castel Volturno: distribution (%) of water-stable aggregate sizes (mm) and stability index (MWD) in different field treatments

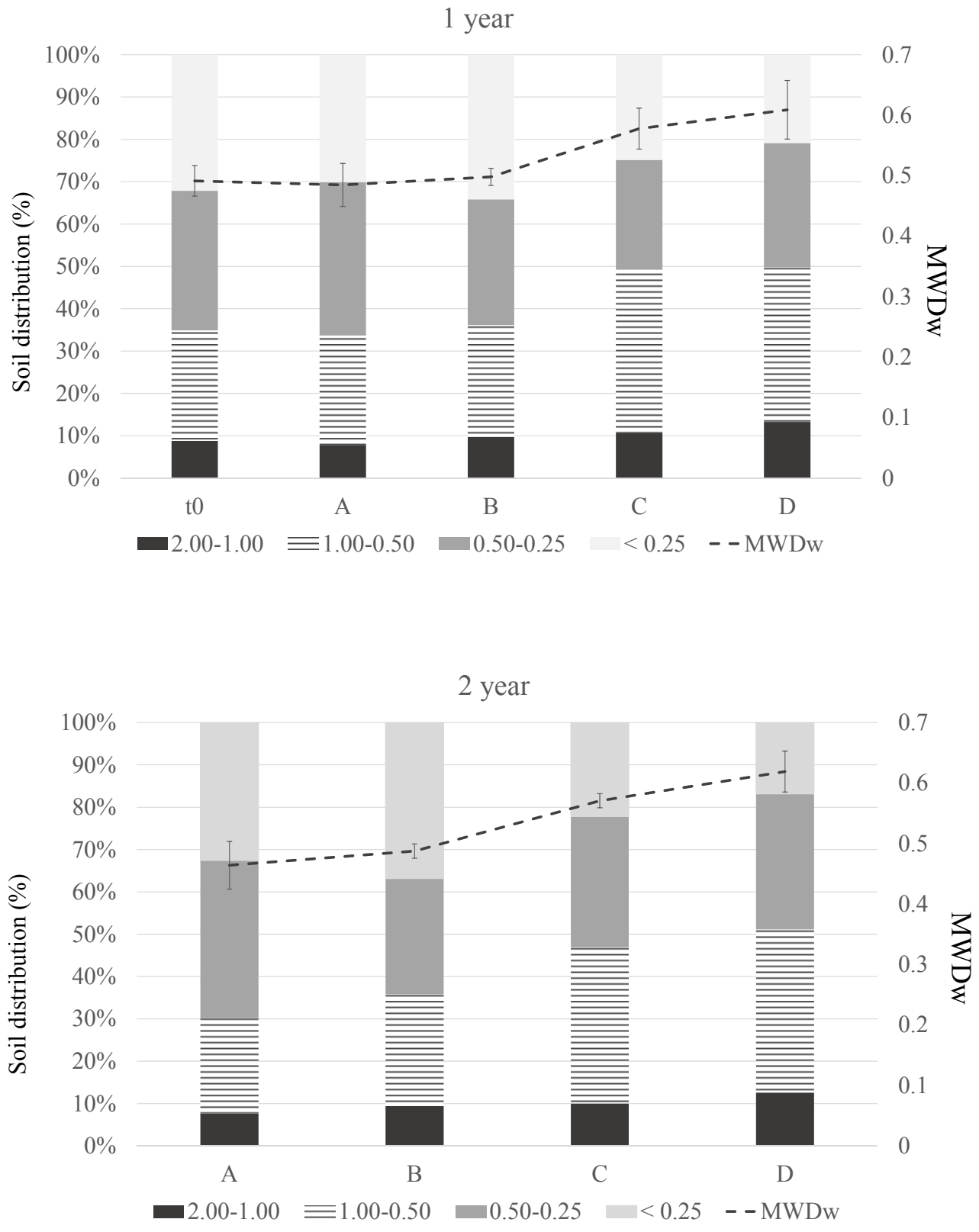

Figure 4 Prima Luce: distribution (%) of water-stable aggregate sizes (mm) and stability index (MWD) in different field treatments

3.2 SOC and N distribution

After two year of SOM managements an average improvement of SOM content was found in field plots with organic amendments of each project sites in respect to conventional managed plots (Figs. 5, 6, 7, 8). The widespread increase of TOC found in different bulk soils ranged from 0.8 to 2.8 g kg-1, depending on soil type and dose of organic amendment, while no relevant differences may be associated with different compost composition. The stable incorporation of OM inputs was confirmed by the OM distribution found in aggregate size fractions which stacked amounts revealed the steady larger OC content in compost amended plots of each field site.

With respect to SOC and N distribution, the lower aggregation capacity of the light textured soils of Tetto Frati and Grandi resulted in a null contribution of larger aggregate sizes (2.0-1-0 mm) to total SOM (Figs. 5, 6)

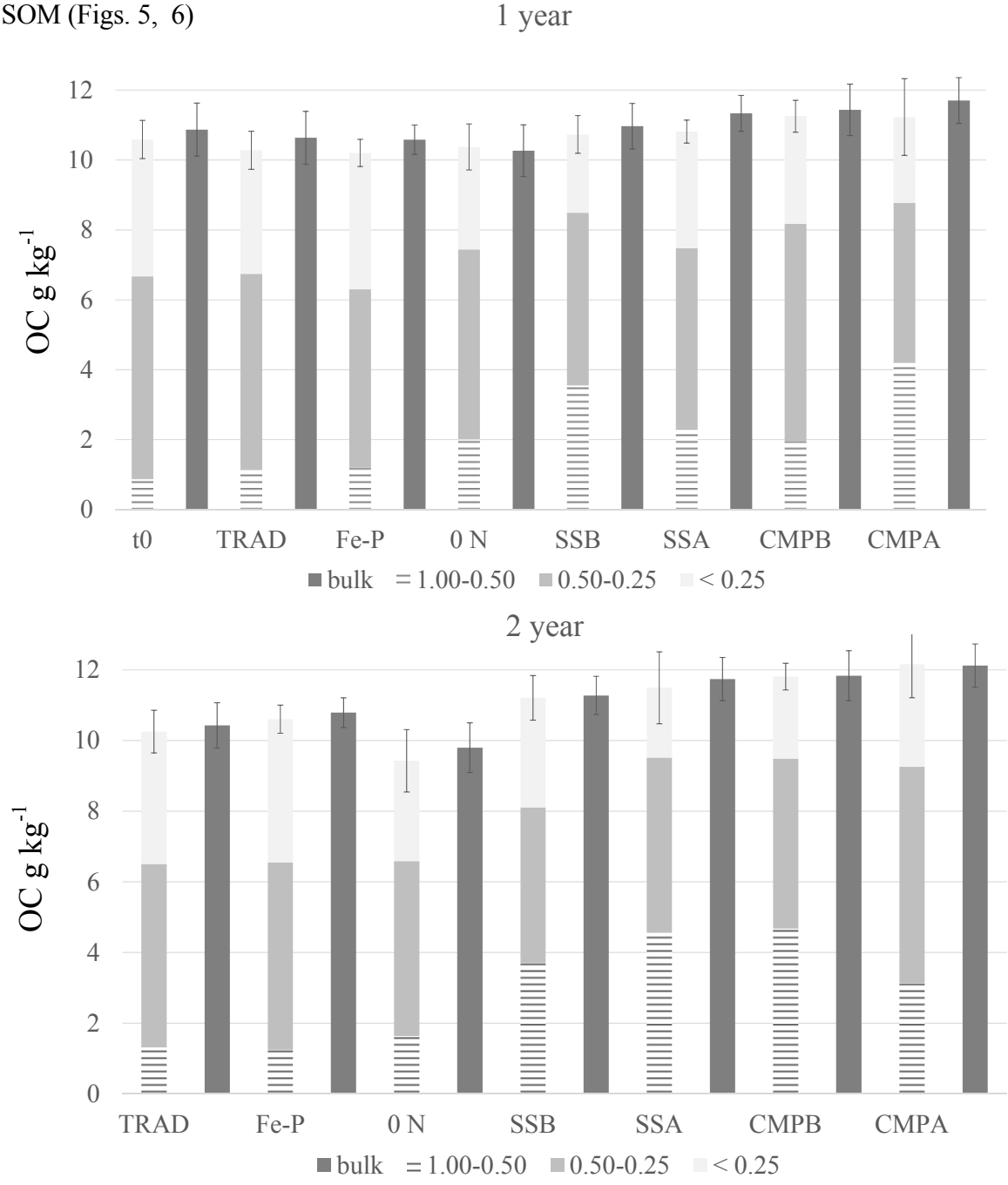

Figure 5a Tetto Frati: SOC content (g kg-1) in bulk soil and aggregates in different treatments

At the end of second year in Tetto Frati farm site, the soil treatments with organic amendments showed an overall increase of about 1-1.2 g OC kg^{-1}, with minor differences among doses and OM types (Fig. 5a). The larger fraction of SOM in amended plots was incorporated in macro-aggregates, thereby supporting the aggregation process observed in aggregate distribution (Fig. 2b). For the N content in bulk soils only the larger dose of compost addition (CMPA) showed a significant increase in respect to control soil. Although not significant, the distribution in aggregated fractions revealed slight larger recovery of N in in soil treatments with organic matter addition, except for the SSA sample (Fig. 6b).

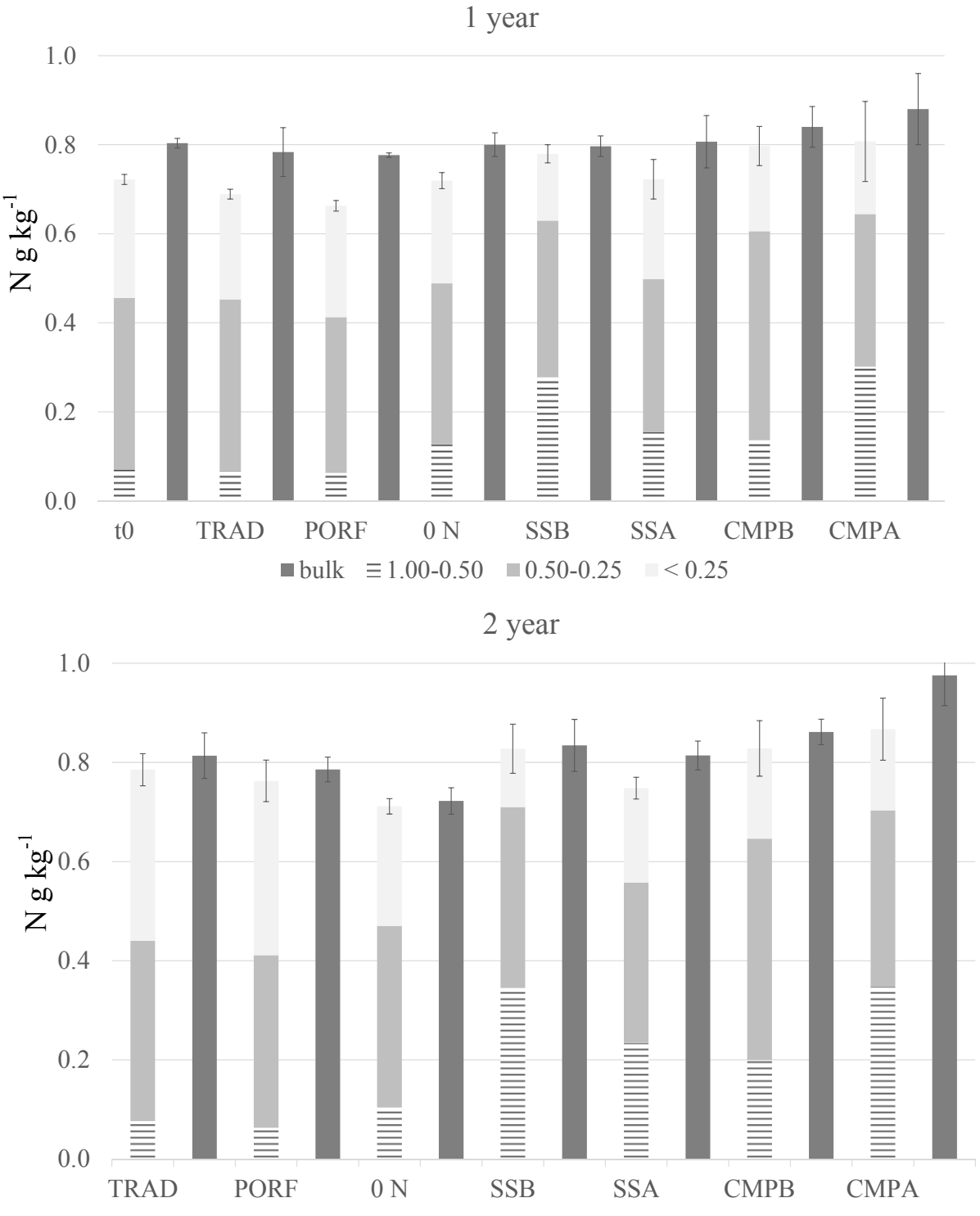

Figure 6b Tetto Frati: total N content (g kg-1) in bulk soil and aggregates in different treatments

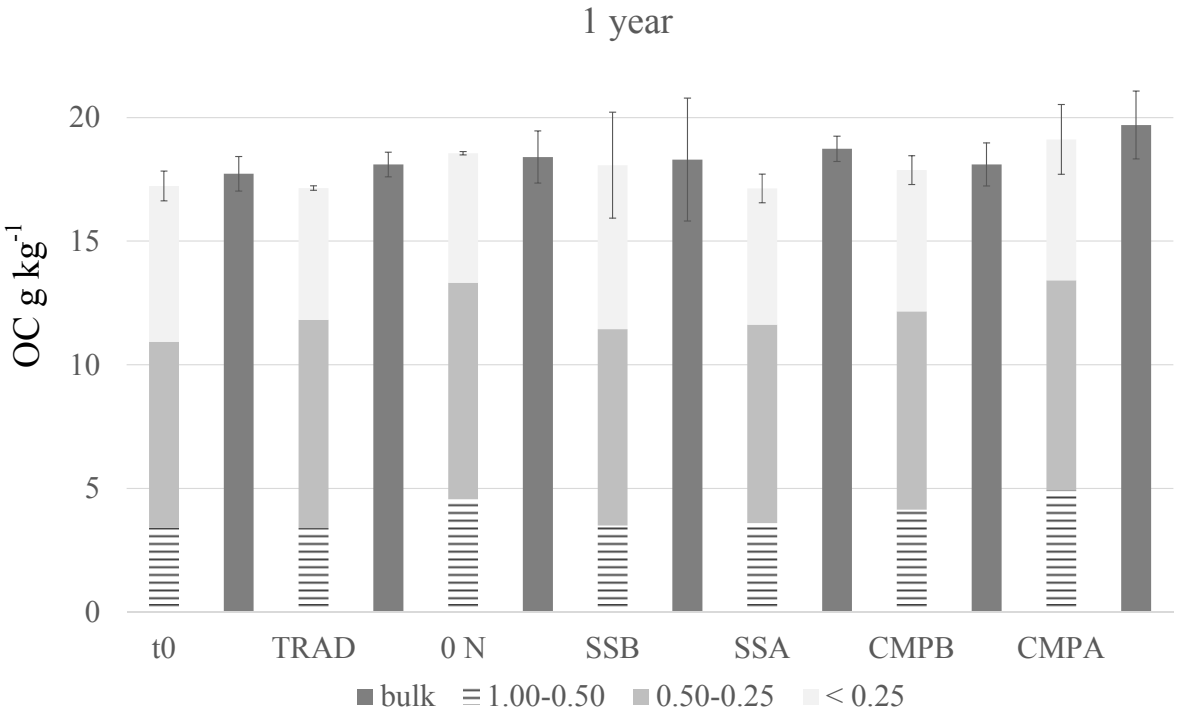

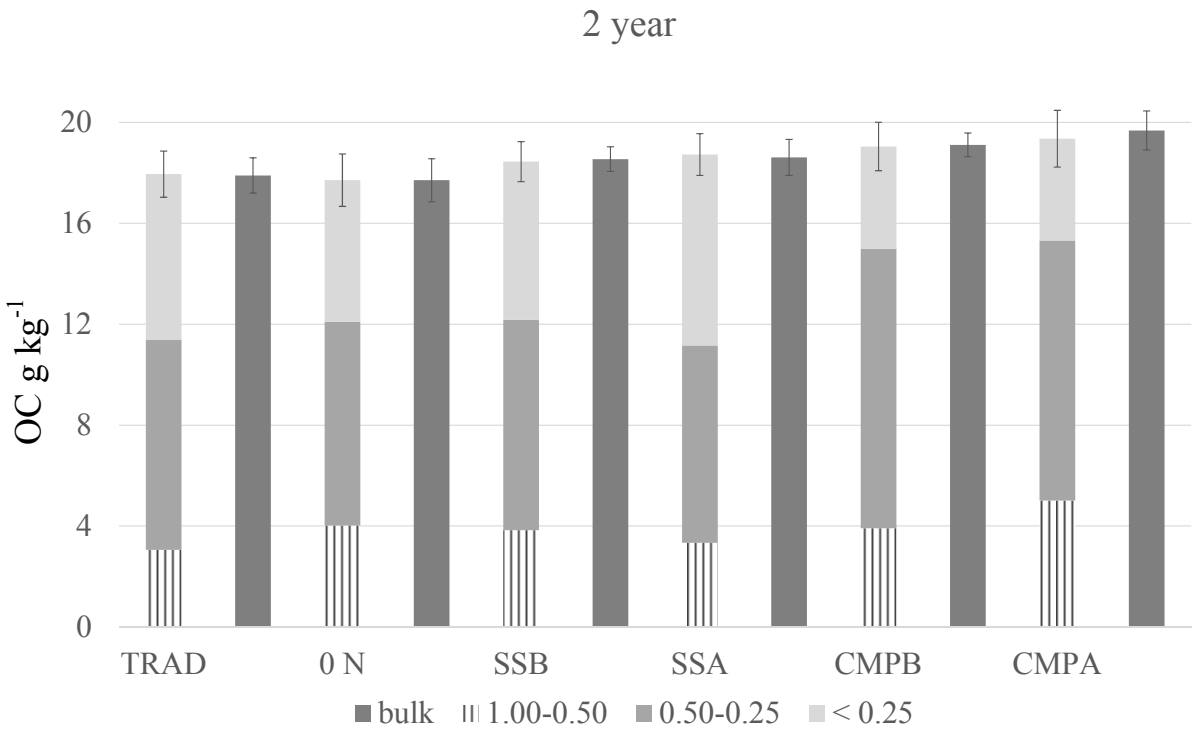

Figure 7a Grandi: total SOC content (g kg-1) in bulk soil and aggregates in different treatments

In the Grandi farm at the end of second crop cycle, the soil treatments with organic matter additions showed an increase in SOC content which ranged from 0.6, to 1.6 g kg^{-1} from SSB to CMPA samples, in both bulk soils and combined size fractions, although not statistical differences were found in respect to traditional plots (Fig 7a). The OC distribution among soil aggregates revealed a large OC partition in finest particles for soil treatment with fresh solid digestate (SSB and SSA),

while more than the 80% of TOC in CMPB and CMPA was incorporated in the water stable macroaggregates (> 0.25 mm).

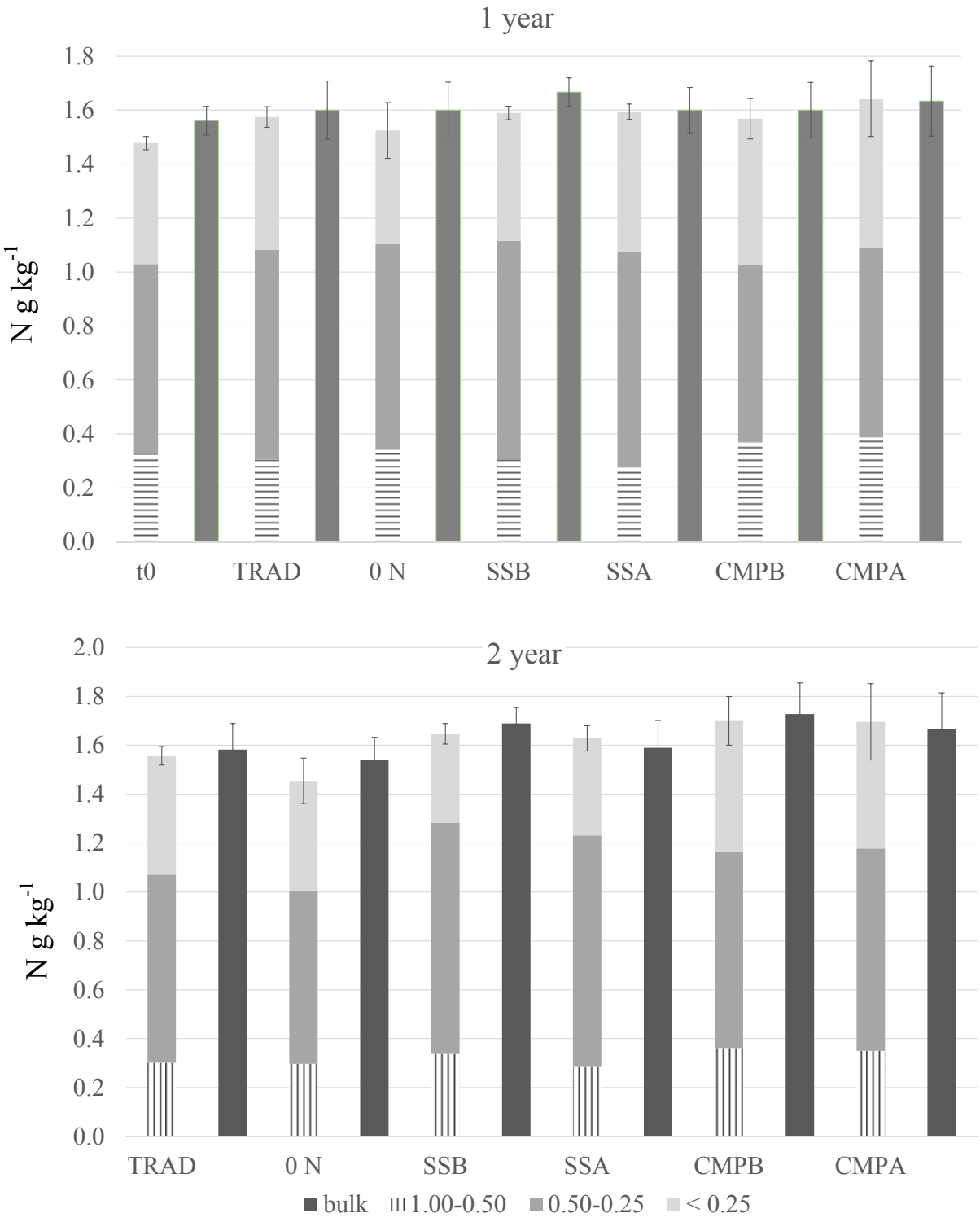

Figure 7b Grandi: total N content (g kg-1) in bulk soil and aggregates in different treatments

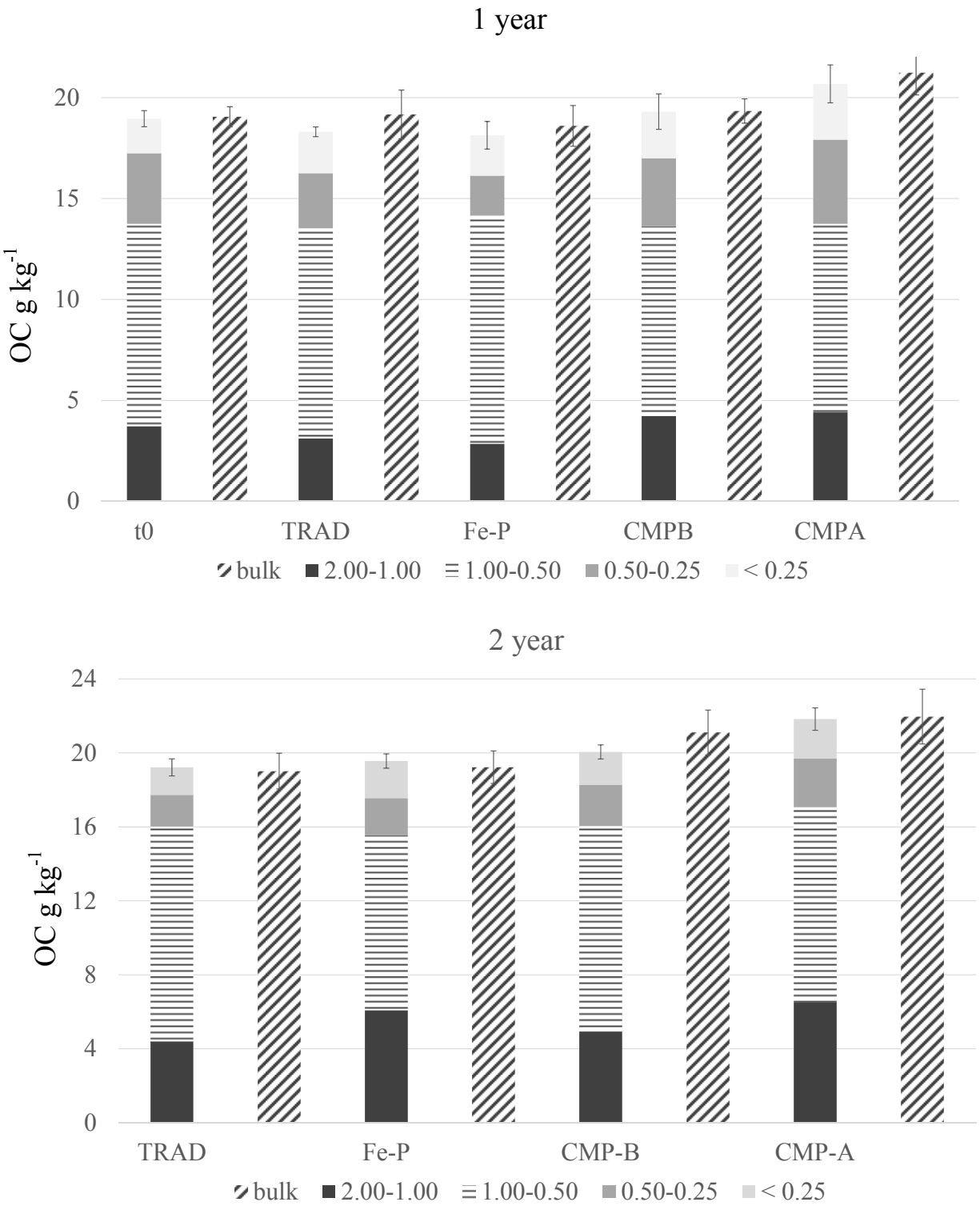

Figure 8a Castel Volturno: total SOC content (g kg-1) in bulk soil and aggregates in different treatments

In the project site of Castel Volturno the TOC content of field plots at the second year, indicated a significant incorporation of exogenous organic materials in soil treatments with on-farm manure compost with an increase of about 2.1 and 2.8 g kg^{-1} for CMPB and CMPA (Fig. 8a). This finding

may be related to the large content finest soil fraction (clay) and the larger aggregation capacity which may have exerted an additional physical protection on the exogenous OM inputs.
As noted for the other soils, slight changes were found in the relative distribution of TOC among soil aggregates, thereby supporting the major influence of textural components in the aggregation processes. Although also the yields of total N content showed a comparable trend (Fig. 7b), both soil treatments with either conventional management and biomimetic catalyst addition underwent to an unusual significant increase in respect to the first year, thereby reducing the gap with compost amended field plots.

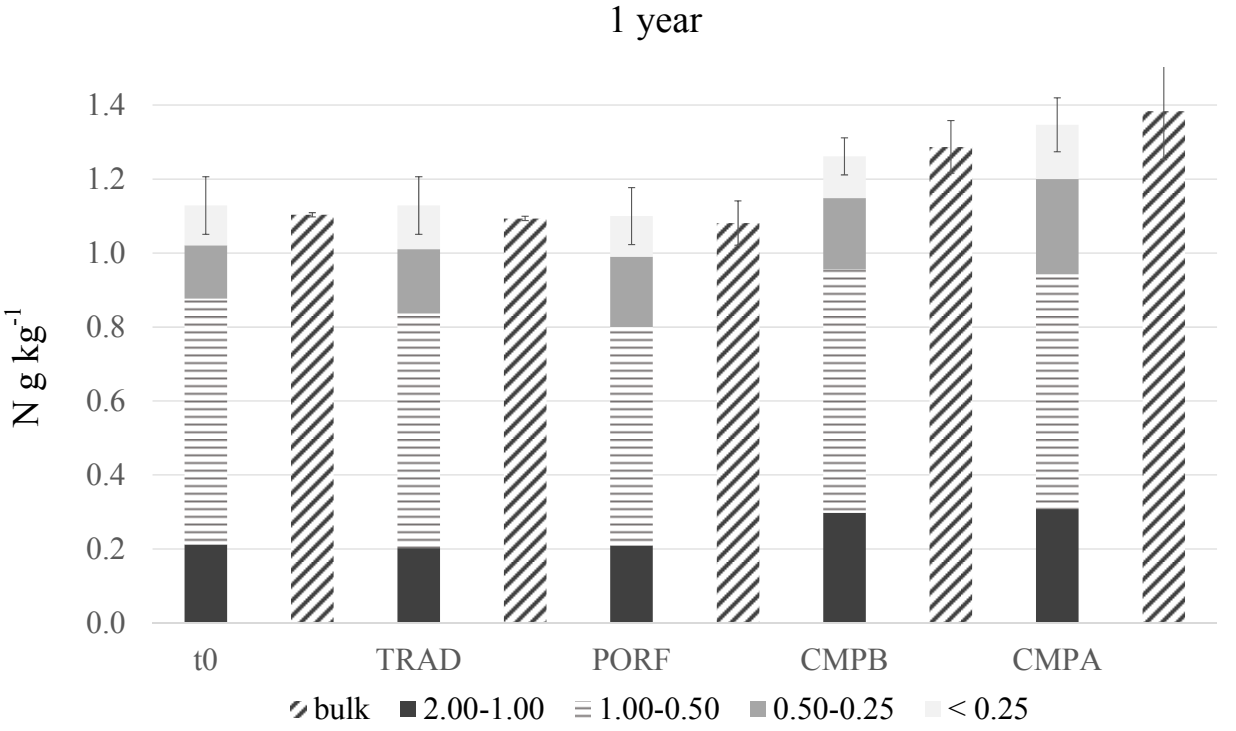

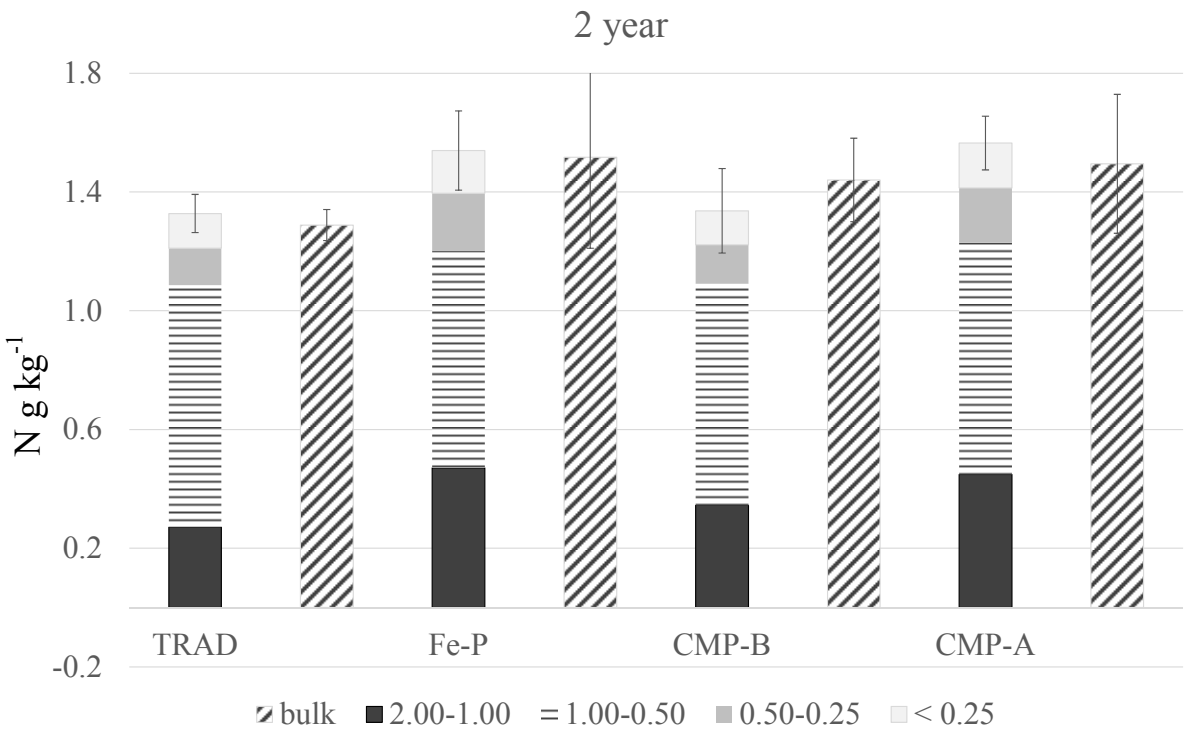

Figure 7b Castel Volturno: total N content (g kg-1) in bulk soil and aggregates in different treatments

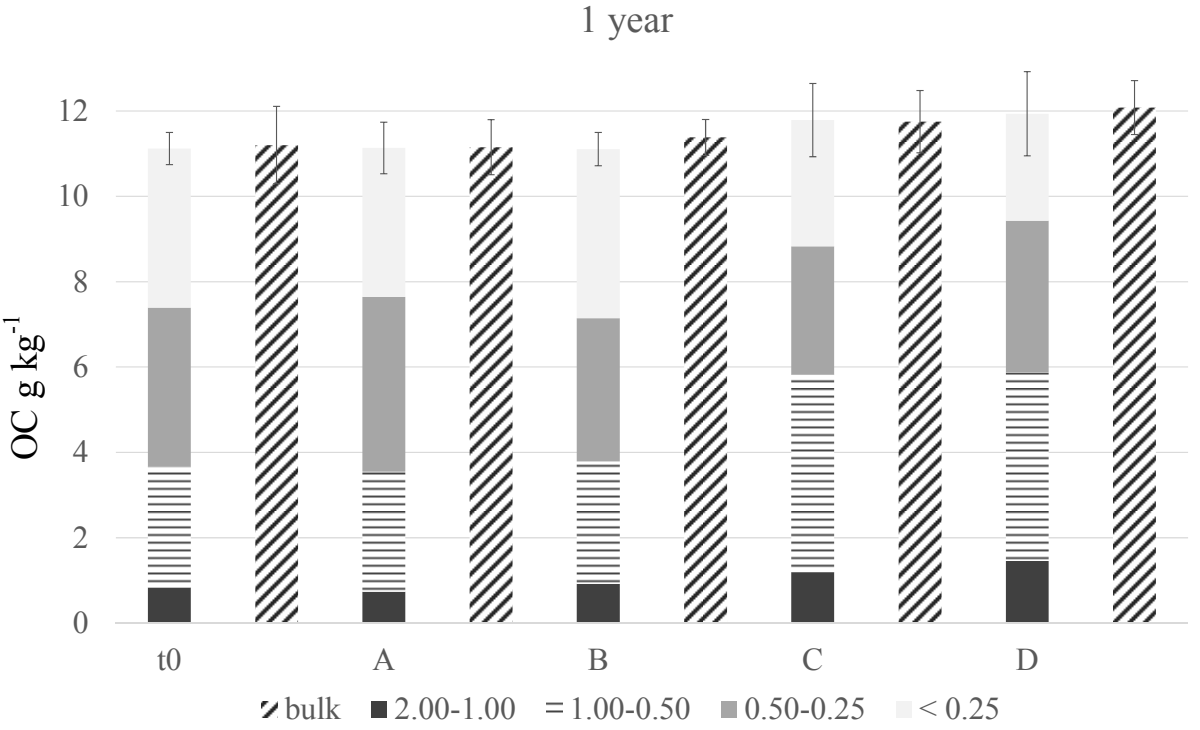

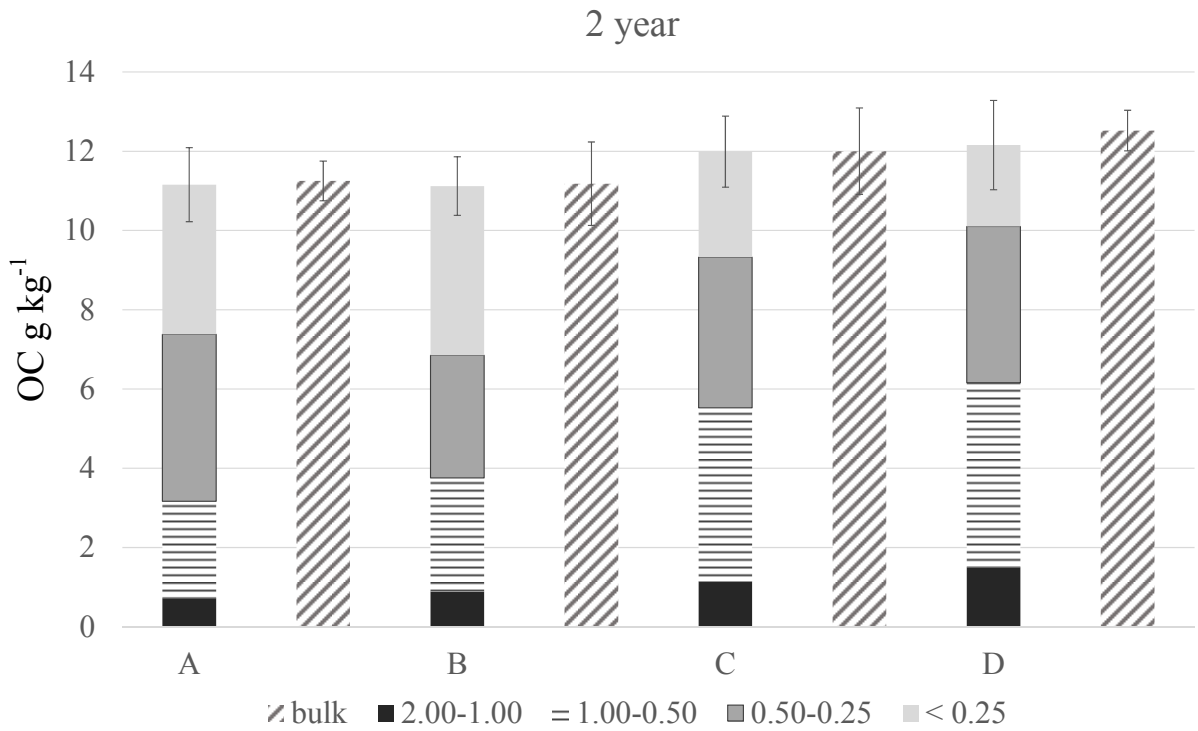

Figure 8a Prima Luce: total SOC content (g kg-1) in bulk soil and aggregates in different treatments

An improvement of SOM content was found in both bulk soils and size-aggregates in field plots amended with on farm compost at the project sites of Prima Luce (Figs 8), which were characterized by an increase of 0.8-1.2 g kg-1 in respect to traditional samples. The incorporation of exogenous OM revealed a combined increase of OC concentration in the lower aggregate classes (< 0.50 mm) and a progressive accumulation of global TOC in larger size fractions of C and D treatments thereby confirming the positive effect of OM addition on the aggregation process.

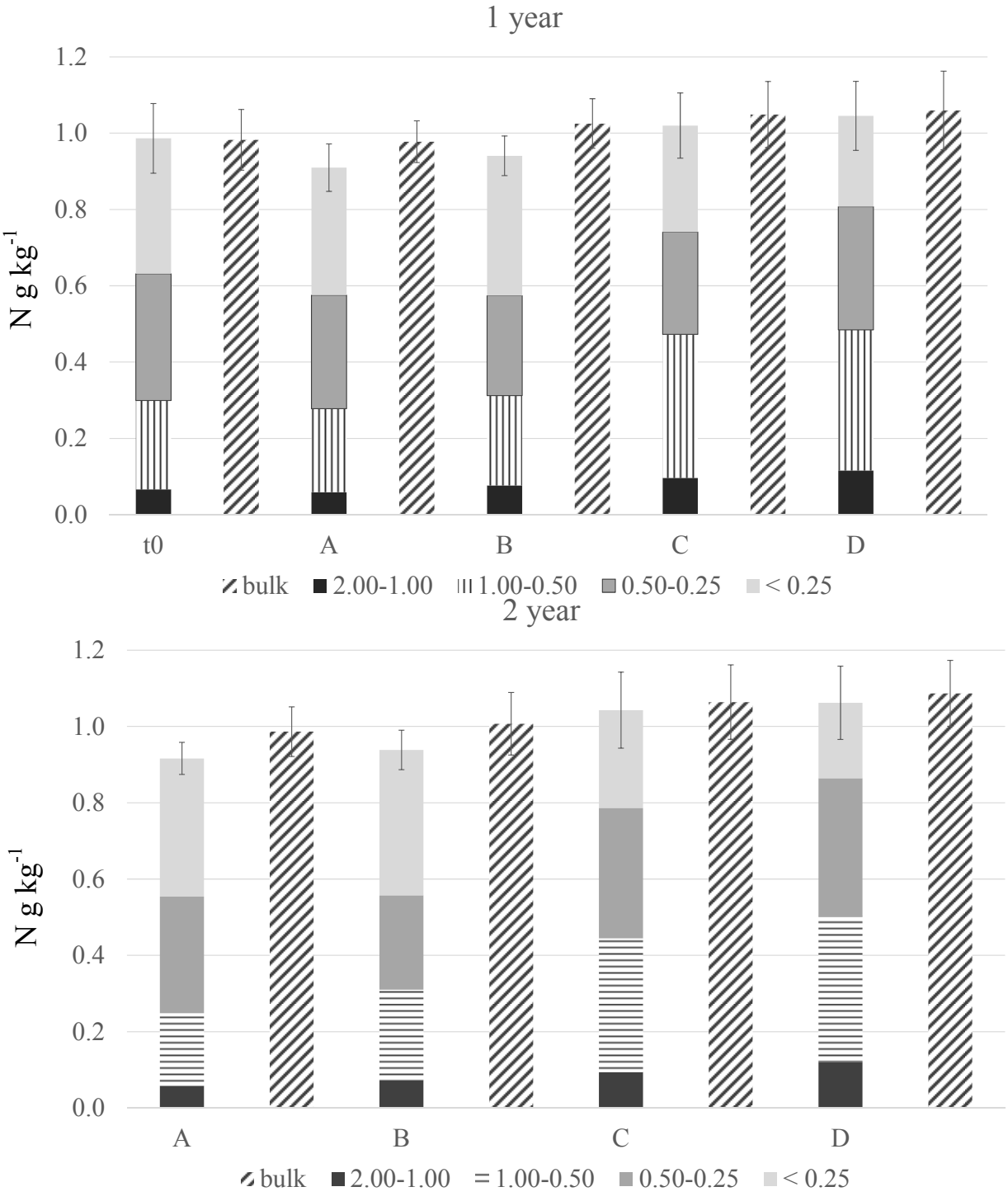

Figure 8b Prima Luce: total N content (g kg-1) in bulk soil and aggregates in different treatments

3.3 13C isotopic content

The analyses of initial isotopic content were performed in the first year of field activities after the distribution of organic materials for the project sites of Tetto Frati, Grandi and Castel Volturno.
The higher isotopic values found in control and organic amended samples in bulk soils and soil aggregates of Tetto Frati (Table 1) highlighted the previous incorporation of 13C labelled OC derived from the long term cultivation of C4 plants (maize) which has provided a natural labelling of SOM pools.

Table 1 13C isotopic ratio measured in organic materials of control and organic amended field plots of different project sites (TF: tetto Frati, G: Grandi, CV: Castel Volturno)

Organic materials	Solid digestate -26.7		Digestate Compost -25.3		Manure compost -23.7	
Treatments	Bulk soil	Soil aggregates				
		2.00-1.00	1.00-0.50	0.50-0.25	<0.25	
TF-Trad	-20.252	/	-19.619	-20.199	-20.694	
TF-SSB	-20.406	/	-20.218	-20.218	-20.698	
TF-SSA	-20.550	/	-20.220	-20.644	-20.676	
TF-CMPB	-20.380	/	-19.857	-20.364	-20.560	
TF-CMPA	-20.512	/	-20.061	-20.472	-20.727	
G-Trad	-24.650	/	-24.836	-24.609	-24.566	
G-SSB	-24.705	/	-25.042	-24.587	-24.603	
G-SSA	-24.615	/	-24.804	-24.541	-24.548	
G-CMPB	-24.626	/	-24.810	-24.552	-24.563	
G-CMPA	-24.598	/	-24.793	-24.518	-24.534	
CV-Trad	-25.079	-25.176	-25.099	-25.123	-25.080	
CV-CMPB	-25.029	-25.128	-25.043	-25.037	-25.068	
CV-CMPA	-24.979	-25.023	-25.019	-25.013	-25.007	

The yield of 13C- OC (% of TOC) deriving from exogenous organic materials in bulk soils, calculated from the isotopic measurements, mostly match the theoretical amounts added with soil treatments (Figs. 10, 11, 12).

In the project site of Tetto Frati the added organic carbon was initially incorporated in soil macro-aggregates for both soil amendments with fresh digestate and compost (Fig. 10). Conversely a more even distribution was found in the project sites of Grandi and Castel Volturno with a fraction of new organic inputs transferred also in the micro-aggregates, even if the13C content of macro-aggregates represented more than the 75% of added organic carbon (Figs 11, 12)

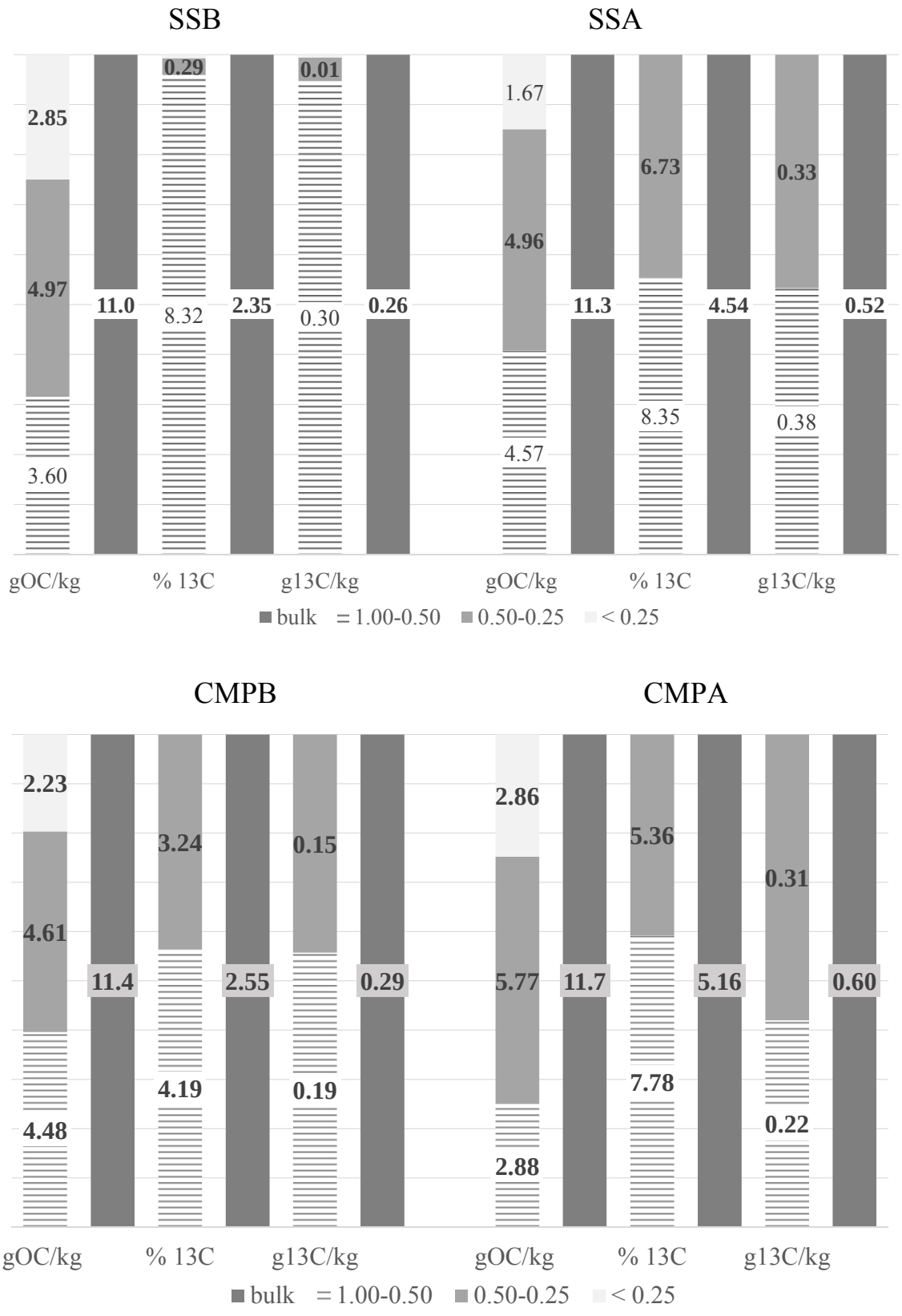

Figure 10 Tetto Frati: 13C-OC content (% and absolute) in bulk soils and aggregates of field amended plots, compared to TOC content

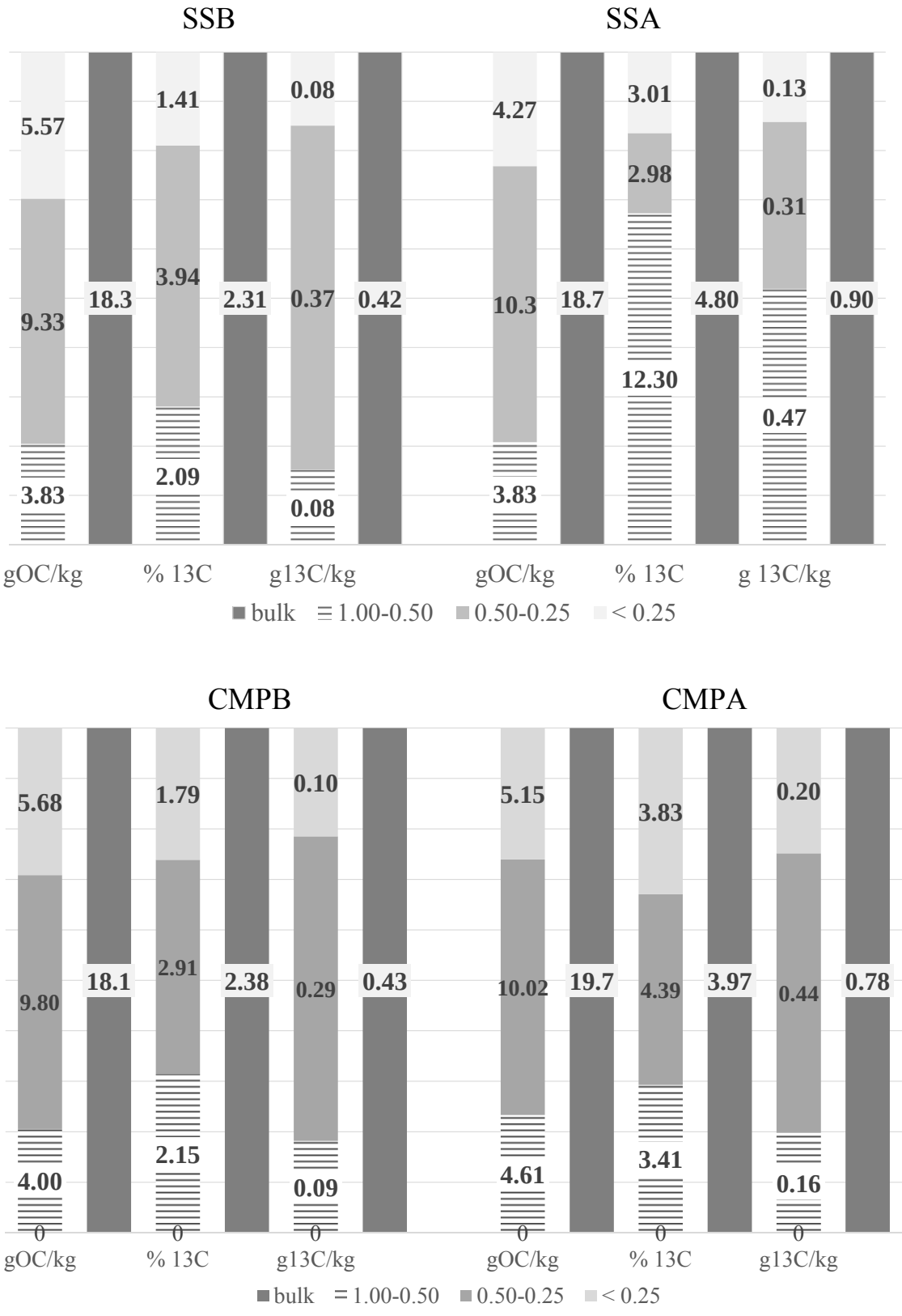

Figure 11 Grandi: 13C-OC content (% and absolute) in bulk soils and aggregates of field amended plots, as compared to TOC content

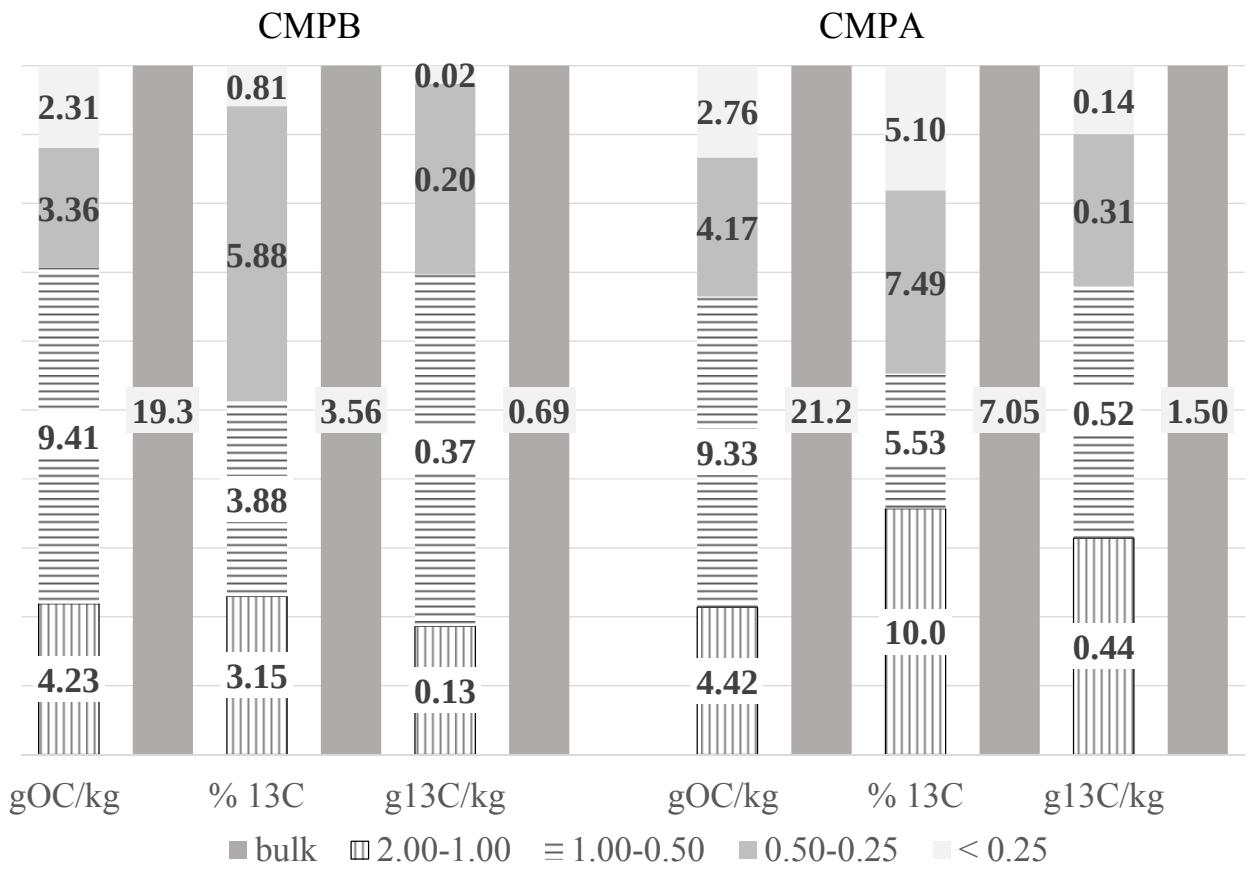

Figure 12 Castel Volturno: 13C-OC content (% and absolute) in bulk soils and aggregates of field amended plots, compared to TOC content

3.4 off line THM-GC-MS

Representative total ion chromatograms (TIC) derived from the thermochemolysis of soil samples from the different project sites of Tetto Frati, Grugliasco, Castel Volturno and Prima Luce are shown in Figure 13 while the compounds identified in the pyrograms are listed in Table 2.

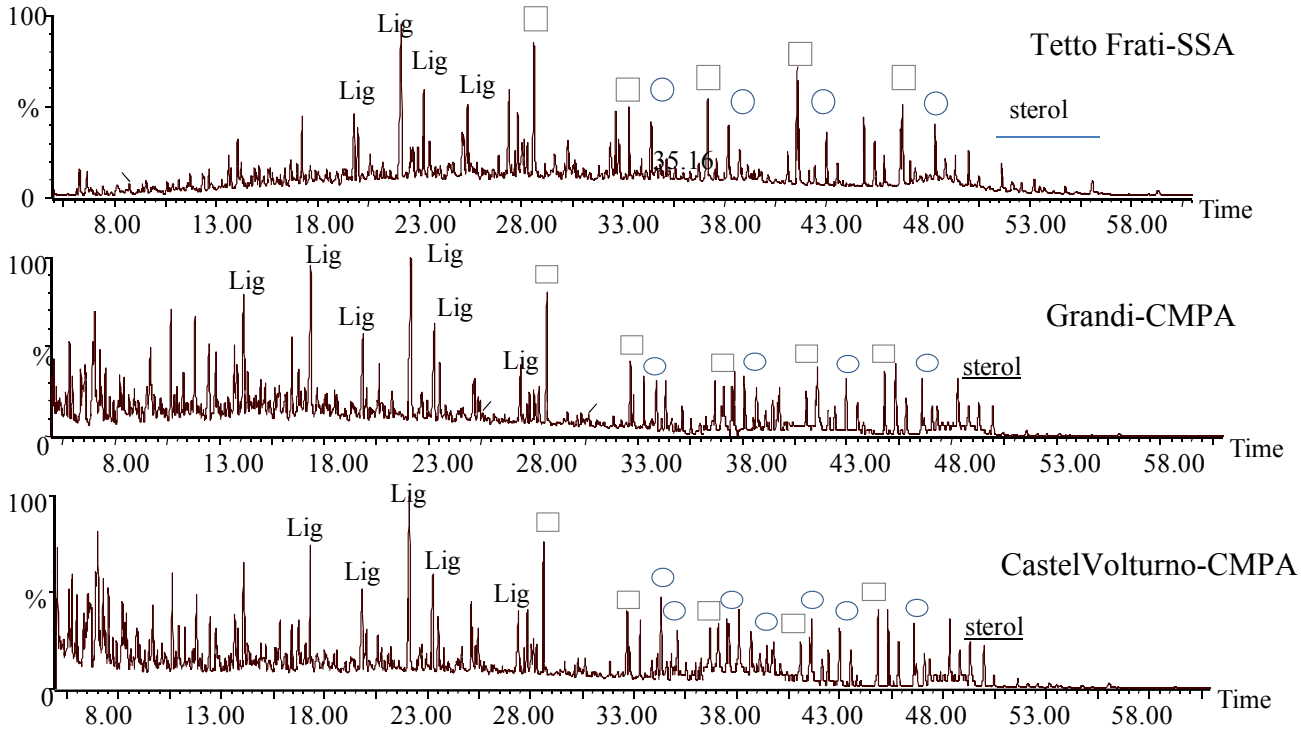

Figure 13 Total ions chromatograms of thermochemolysis products released from soils samples: Lg Lignin, □ Fatty acids, ○ Biopolyesters (alkyl-dioic acids, hydroxyl acids)

The thermochemolysis released more than hundred recognizable different molecules, which were identified as methyl ethers and esters of natural compounds (Tab. 2). The majority of these compounds originated from higher plants and microbial by-products and was represented by lignin components, fatty acids, aliphatic biopolymers, hydrocarbons and alcohols. The large yield of TAHM GC-MS products enabled a feasible quantitative determination of the organic compounds (Tabs. 3, 4, 5, 6). The lignin monomers released by the field plots are inherited from the structural components which build up the lignified tissues of higher plants. The specific compounds have been determined by the main fragmentation pattern and were associated to the current symbols used to distinguish the different structural units: P p-hydroxyphenyl, G guaiacyl (3-methoxy, 4-hydroxyphenyl), and S syringyl (3,5-dimethoxy, 4-hydroxyphenyl). The lignin molecules found in initial soil samples (Tab. 2) indicated the presence of, both, fresh decaying plant residues and that of microbial processed organic materials. The latter derivatives included the oxidized products of both di- and tri-methoxy phenylpropane molecules, with the aldehydic (G4, S4), ketonic (G5, S5) and benzoic-acid (G6, S6) forms as main components.

Table2 List of thermochemolysis products[a] released from initial soil samples

RT[a]	assignment [b]	characteristic ions m/z
5.4	1-Methyl 4-CH_3O Benzene *Lg P2*	77, 91, 107 M^+122
8.5	Benzene, 1,2-di CH_3O *Lg G1*	77, 95, 123 M^+138
8.8	Carbohydrate derivative	88, 101, 130 M^+nd
11.9	Carbohydrate derivative	88, 101, 130 M^+nd
12.5	Carbohydrate derivative	101, 129, 161 M^+nd
12.7	1,3,5-tri CH_3O Benzene	125, 153 M^+168
13.1	C10 Fame	74, 87, 155 M^+ 186
13.6	N Compound	98 M^+nd
14.5	1,2,3-tri CH_3O Benzene *Lg S1*	110, 125, 153 M^+168
14.6	Benzoic Acid, 4- CH_3O ME *Lg P6*	77, 92, 135 M^+166
14.9	Carbohydrate derivative	88, 101, 143, 175 M^+nd
15.1	Carbohydrate derivative	88, 101, 143, 175, 188 M^+nd
17.2	Carbohydrate derivative	88, 101, 130 M^+nd
17.6	Benzaldehyde, 3,4-di CH_3O *Lg G4*	151, 165 M^+166
17.7	Carbohydrate derivative	88, 101, 175 M^+nd
18.2	Carbohydrate derivative	101, 129, 161 M^+nd
18.5	Carbohydrate derivative	101, 129, 161 M^+nd
18.8	C12 FAME	74, 87, 183 M^+ 214
19.9	3,4 di CH_3O Acetophenone *Lg G5*	137, 165, M^+180
20.7	Benzoic Acid, 3,4-di CH_3O, ME *Lg G6*	165, 181, M^+196
20.9	Benzaldehyde, 3,4,5-tri CH_3O *Lg S4*	125, 181, M^+196
21.6	cis -2-(3,4-di CH_3O phenyl)-1-CH_3O ethylene *Lg G7*	151, 179 M^+194
21.9	trans -2-(3,4-di CH_3O phenyl)-1- CH_3O ethylene *Lg G8*	151, 179, M^+194
22.2	cis-1-Methoxy-1-(3,4-di CH_3O phenyl)-1-Propene *Lg G10*	165, 193 M^+208
23.0	trans -3-(4-CH_3O phenyl)-3-Propenoic acid ME *Lg P18*	133, 161 M^+ 192
23.0	trans-1-Methoxy-1-(3,4-di CH_3O phenyl)-1-Propene *Lg G11*	165, 193 M^+208
23.9	N compound	98 M^+nd
24.1	Benzoic Acid, 3,4,5-Trimethoxy ME *Lg S6*	195, 211 M^+226
24.3	C14 FAME	74, 87, 211 M^+ 242
24.6	trans-3- CH_3O -1-(3,4-di CH_3O phenyl)-1-Propene *Lg G13*	91, 177 M^+208
25.5	cis-1-(3,4,5-tri CH_3O phenyl)-1- CH_3O ethylene *Lg S10*	195, 223 M^+238
25.9	Thr/Eryth-1-(3,4-di CH_3O phenyl) -1,2,3-tri CH_3O propane *Lg G14*	166, 181 M^+270
25.9	C15 *iso* FAME *Mic-PLFA*	74, 87, 213 M^+256
26.0	trans-1-(3,4,5-tri CH_3O phenyl)-1- CH_3O ethylene *Lg S11*	195, 223 M^+238
26.1	C15 *anteiso* FAME *Mic-PLFA*	74, 87, 213 M^+256
26.2	Thr/Eryth.-1-(3,4-di CH_3O phenyl) -1,2,3-tri CH_3O propane *Lg G15*	166, 181 M^+270
26.5	cis-1- CH_3O-1-(3,4,5-tri CH_3O phenyl)-1-Propene *Lg S13*	91, 207 M^+238
26.8	C15 *n*-FAME	74, 87, 225 M^+256
28.3	2-Propenoic Acid, 3-(3,4-di phenyl)-, ME *Lg G18*	191, 207 M^+222
28.4	C16 *iso* FAME *Mic-PLFA*	74, 87, 227 M^+270
28.6	Thr./Eryth-1-(3,4,5-tri CH_3O phenyl) -1,2,3-tri CH_3O propane *Lg S14*	181, 211 M^+300
28.8	C16:1 FAME *Mic-PLFA*	55, 74, 236 M^+268

Table 2 continue

RT[a]	assignment[b]	characteristic ions m/z
28.9	Thr./Eryth-1-(3,4,5-tri CH_3O phenyl) -1,2,3-tri CH_3O propane *Lg S15*	181, 211,M^+300
29.0	C16:1 FAME	55, 74, 236 M^+268
29.4	C16 FAME	55, 74, 239 M^+270
30.4	7 methyl C16FAME *Mic-PLFA*	74, 87, 157 M^+284
30.6	Carbohydrates derivative	88, 101, 115, 175, 235 M^+nd
30.7	cis-3-(3,4,5-tri CH_3O phenyl-3-Propenoic acid ME *Lg S18*	221, 237 M^+252
30.8	C17 *iso* FAME *Mic-PLFA*	74, 87, 241 M^+284
31.0	C17 *anteiso* FAME *Mic-PLFA*	74, 87, 227 M^+284
31.2	trans-3-(3,4,5-tri CH_3O phenyl-3-Propenoic acid ME *Lg S18*	221, 237 M^+252
31.4	C17 cy FAME *Mic-PLFA*	55, 69, 250 M^+282
31.6	cis-1-(3,4,5-tri CH_3O phenyl) -1,3-di CH_3O prop-1-ene *Lg S16*	206, 237 M^+268
31.8	C17 *n*-FAME	74, 87, 253 M^+284
33.4	C18 *iso* FAME *Mic-PLFA*	74, 87, 253 M^+298
33.5	C18:1 FAME	55, 69 264 M^+296
34.0	C18 FAME	74, 87 267 M^+298
34.6	16, 16-CH_3O, FAME	55, 74, 268, 285 M^+300
34.9	C18, 10 CH_3O, FAME	55, 69, 183, 215, 297 M^+328
36.3	Carbohydrates derivative	88, 101, 187, 219, 423 M^+nd
36.7	C16 Dioic Acid DIME	74, 98, 241, 283 M^+314
37.4	C16, 8(9,10)-16 diCH_3O, FAME	71, 95, 87, 201, 215 M^+330
37.9	Carbohydrates derivative	88, 101, 187, 279, 423 M^+nd
38.1	C18:1, 18 CH3O, FAME	55, 67, 81, 262, 294 M^+326
38.3	C20 FAME	74, 87, 295 M^+326
38.8	Carbohydrates derivative	88, 101, 187, 219, 359 M^+nd
39.8	C24 Alkane	57, 71, 85, M^+338
40.2	Carbohydrates derivative	88, 101, 111, 187, 391 M^+nd
40.3	C21 FAME	74, 87, 309 M^+340
40.6	C22-CH_3O	57, 69, 83, 318, M^+340
40.8	C18 Dioic acid DIME	74, 98, 241, 311 M^+342
41.1	Carbohydrates derivative	88, 101, 145, 187, 279 M^+nd M^+nd
41.7	C25 Alkane	57, 71, 85, M^+352
42.3	C22 FAME	74, 87, 323 M^+354
42.5	Carbohydrate derivative	88, 101, 187, 219, 279, 423 M^+nd
42.6	Carbohydrate derivative	88, 101, 111, 187, 391 M^+nd
42.8	C20, 20 CH_3O, FAME	55, 74, 292, 324, M^+356
43.1	C18 9, 10, 18 tri CH_3O FAME	71, 81, 169, 187, 201 M^+388
43.6	C26 Alkane	57, 71, 85, M^+366
44.2	C23 FAME	74, 87, 337 M^+368
44.4	C24-CH_3O	57, 69, 83, 346, M^+368
44.6	C22, 2 CH_3O, FAME *Mic*	57, 71, 97, 325 M^+384
45.0	C20 Dioic Acid DIME	74, 98, 241, 339 M^+370

Table 2 continue

RT[a]	assignment[b]	characterisitc ions m/z
45.4	C27 Alkane	57, 71, 85, M^+380
46.0	C24 FAME	74, 87, 351 M^+382
46.2	C23, 2 CH_3O, FAME *Mic*	57, 71, 97, 339 M^+398
46.5	C22, 22 CH_3O, FAME	55, 74, 320, 352 M^+384
47.2	C28 Alkane	57, 71, 85, M^+394
47.4	squalene	69, 81, 136, 341 M^+410
47.7	C25 FAME	74, 87, 365 M^+396
47.9	C26-CH_3O	57, 69, 83, 364, M^+396
48.0	C24, 2 CH_3O, FAME *Mic*	57, 71, 97, 353 M^+412
48.2	C22 Dioic acid DIME	74, 98, 241, 367 M^+398
48.9	C29 Alkane	57, 71, 85, M^+408
49.4	C26 FAME	74, 87, 379 M^+410
49.6	C25, 2 CH_3O, FAME *Mic*	57, 71, 97, 367 M^+426
49.9	C24, 24 CH3O, FAME	55, 74, 348, 380 M^+412
50.5	C30 Alkane	57, 71, 85, M^+422
51.0	C28-CH_3O	57, 69, 83, 392, M^+424
51.2	C26, 2 CH_3O, FAME *Mic*	57, 71, 97, 381 M^+440
51.5	C24 Dioic acid DIME	74, 98, 241, 395 M^+426
51.7	Phytosterol (tetracyclic)	213, 255, 289, 382 M^+414
52.1	C31 Alkane	57, 71, 85, M^+426
52.4	Phytosterol (tetracyclic)	213, 255, 329, 396 M^+428
52.6	C28 FAME	74, 87, 407 M^+438
52.8	Phytosterol (tetracyclic)	213, 273, 329, 396 M^+428
53.1	C26, 26 CH3O, FAME	55, 74, 376, 408 M^+440
53.4	Phytosterol (tetracyclic)	215, 233, 257, 398 M^+430
53.7	Triterpenol (pentacyclcic)	189, 203, 262 M^+nd
54.0	C30-CH_3O	57, 69, 83, 420, M^+452
54.2	Triterpenol (pentacyclcic)	5, 218, 275, 410 M^+442
54.5	Triterpenol (pentacyclcic)	204, 218, 301, 316 M^+440
55.0	Triterpenol (pentacyclcic)	204, 248, 394 M^+454

a. RT = Retention Time (minutes)

b. cy=cyclopropane; CH_3O = Methoxy; DIME = dimethyl ester; FAME= fatty acid methyl ester; Lg=lignin; ME = methyl ester; Mic=microbial; nd=not determined

Conversely the concomitant release from the thermochemolysis of soil samples, of 1-(3,4-dimethoxyphenyl)-1(3)-methoxy-propene (G10/11, G13) and 1-(3,4,5-trimethoxyphenyl)- 1(3)-methoxy-propene (S10/11, S13), as either cis or trans isomers (Tab.2), may be related to the incorporation on SOM of slightly decomposed plant debris.

Moreover the identification of the enantiomers of 1-(3,4-dimethoxyphenyl)-1,2,3-trimethoxypropane (G14 and G15) and 1-(3,4,5- trimethoxyphenyl)-1,2,3-trimethoxypropane (S14 and S15), confirmed the persistence of not decomposed lignified plant tissues. The aldehydic and acidic forms of guaiacyl and syringyl structures result from the progressive oxidation of lignin

monomers, while the corresponding homologues holding methoxylated side chains are indicative of unaltered lignin components, which retain the propyl ether intermolecular linkages. The Ad/Al index is the ratio of peak areas of acidic structures over those of the corresponding aldehydes (G6/G4, S6/S4), while the Γ index is the ratio of peak areas of acidic structures over the sum of peak areas for the threo/erythro isomers (Γ_G = G6/[G14+G15]; Γ_S = S6/[S14+S15]). Both these indices are considered useful indicators of the bio-oxidative transformation of lignin components. The overall larger values found in the initial samples for the majority of the structural indexes (Tab. 3) indicated the prevalence of decomposed lignin monomers. Among the last eluted lignin monomers, the 3-(4,5-dimethoxyphenyl)-2-propenoic (G18) and the 3-(3,4,5-trimethoxyphenyl)-2-propenoic (S18) acid forms, may have originated from either the side chain oxidation of guaiacyl and siringyl units or from the partial decomposition of aromatic domains of suberin biopolymers in plant tissues.

The various alkyl molecules found in the pyrograms, were mainly composed by aliphatic and alicyclic lipid compounds of plant and microbial origin (Tab.2). The most abundant compounds were the methyl ester of linear fatty acids, dominated by the hexadecanoic and octadecanoic saturated and unsaturated homologues. Notwithstanding the multiple possible origins of the C16 and C18 acids, the predominance of even carbon atoms, indicated the plant waxes as prevalent source of the straight chain aliphatic acids. These compounds may derive from the breakdown of long chain ester as well as from the terminal oxidation of other components such as linear hydrocarbons and aliphatic alcohols. The prevailing role of plant input in soil lipid composition was also suggested by the detection of the C24, C26 and C28 aliphatic alcohols (Tab. 2), which are common components of wax layer of non-lignified tissues. This finding was confirmed by the observed distribution of long-chain hydrocarbons (Tab. 2), marked by the peculiar prevalence of heavier odd-numbered alkanes. The off-line pyrolysis, produced also a notable yield of the methylated form of ω-hydroxy alkanoic acids and alkan-dioic acids (Tabs. 2 and 3).

These molecules are the main constituents of the external protective barriers of fresh and lignified plant tissues, namely cutin and suberin. No clear predominance of particular monomer was revealed by both of these compound classes, which instead showed an almost uniform distribution of even carbon-numbered long chain components (Tab. 2). The 9,16-/10,16-dihydroxyhexadecanoic isomers, and the 9,10 epoxide 18 hydroxy-octadecanoic (Tab. 2) acid were the most abundant representative monomers of mid-chain hydroxyl acids, structural units of plant cuticles, frequently used also as plant biomarkers. The relatively least abundant lipid compounds were the high molecular weight tetra- and pentacyclic triterpenes (Tabs.2 and 3). The sterol and triterpenol molecules have been tentatively identified as methyl ethers and esters of both methyl/ethyl cholesten-3-ol structures, and of ursane, lupeane and oleanane derivatives that are characteristic lipid components of aerial and root plant tissues.

The contribution of microbial input to soil lipids was shown by the inclusion of various structural components of microbial cells, such as phospho-lipid fatty acids (PLFA) and 2-hydroxy aliphatic acids (Tab. 2). The most representative PLFA monomers were, in order of elution, the 12- and 13-methyl tetradecanoic (iso/anteiso pentadecanoic), the 14- and 15-methyl hexadecanoic (iso/anteiso heptadecanoic) acids and the cyclopropane-(2-hexyl)-octanoic acid (C17 cy FAME), which are common microbial constituents of natural organic matter in soil and sediments .

A relative lower amount of carbohydrates derivatives were found among the pyrolysis products of the field management from Torino soil. This finding has been related to the lower efficiency of off-

line pyrolysis techniques to detect carbohydrate units of polysaccharides in complex matrices. The thermal behaviour and pyrolitic rearrangement of poly-hydroxy compounds combined with the basic reaction condition of TMAH reagent solution, are believed to negatively interfere in the release of polysaccharides. However, despite the expected low response of carbohydrates, various methylated forms of mono- and oligo-saccharides components were still found among thermochemolysis products. These compounds may be mainly associated to xylans and cellulose moieties of coarse ligno-cellulosic debris of plant residues.

After two year of SOM managements the soil addition with organic materials produced an overall increase in the yields of both aliphatic and lignin components in all the project sites, thereby confirming the incorporation of exogenous OC in soil samples (Tabs. 3, 4, 5, 6). Moreover the inclusion of stabilized OM was indicated by the progressive decrease of structural indices (Ad/Al, Γ) associated with lignin monomers in compost amended plots. This finding further highlight the modification of SOM quality promoted by the soil treatments

Table 3 Composition[a] and yields (μg g^{-1}) of main TAHM products released from the field plots of Tetto Frati project site

	Compounds	t0	Trad	0N	FeP	SSB	SSA	CMPB	CMPA
				1 year					
Lipids	Fatty acids C_{12}÷C_{28}	3063	3040	2970	3110	3150	3250	3190	3210
	Microbial (%)	7	6	6	5	8	9	8	10
	Mid-chain hydroxy acids C_{16}, C_{18}	172	164	148	154	190	215	210	220
	ω-Hydroxy acids C_{16}÷C_{22}	263	255	266	247	282	291	270	314
	Alkanes C_{25}÷C_{31}	89	78	65	95	85	95	110	100
	Alcohols C_{16}-C_{26}	120	125	115	119	125	125	132	135
	Phytosterols	42	35	40	50	60	65	70	80
	Total lipids	3749	3692	3598	3768	3890	4040	3982	4055
Lignin	Guaiacyl	127	130	125	140	150	180	195	210
	$(Ad/Al)_G$[b]	4.4	4.3	4.5	4.7	4.0	4.1	4.1	4.0
	(Γ_G)[b]	3.0	3.1	2.8	3.1	2.8	2.8	2.8	2.7
	p-Hydroxyphenyl	64	55	67	60	70	58	65	72
	Syringyl	174	190	185	170	164	190	200	210
	$(Ad/Al)_S$[b]	3.5	3.4	3.1	3.6	3.0	3.2	3.2	3.1
	(Γ_S)[b]	3.8	3.7	4.0	3.9	3.6	3.5	4.0	3.7
	Total lignin	365	375	377	370	384	428	460	492
				2 year					
Lipids	Fatty acids C_{12}÷C_{28}		2950	3020	2990	3190	3220	3330	3410
	Microbial (%)		7	7	5	7	9	10	10
	Mid-chain hydroxy acids C_{16}, C_{18}		154	98	145	183	227	235	244
	ω-Hydroxy acids		255	215	200	277	313	291	309
	Alkanes C_{25}÷C_{31}		75	60	80	95	85	100	120
	Alcohols C_{16}-C_{26}		122	105	87	142	85	132	135
	Phytosterols		42	38	46	47	68	74	82
	Total lipids		3598	3536	3548	3934	3998	4162	4200

Lignin	Guaiacyl	142	128	118	147	187	205	310
	$(Ad/Al)_G$[b]	4.3	4.2	4.1	4.0	3.9	3.9	4.0
	(Γ_G)[b]	3.2	3.0	3.1	2.8	2.9	2.8	2.7
	p-Hydroxyphenyl	58	55	64	72	71	74	80
	Syringyl	185	174	177	202	215	208	215
	$(Ad/Al)_S$[b]	3.4	3.5	3.4	3.0	3.1	3.1	3.1
	(Γ_S)[b]	3.9	4.1	3.7	3.6	3.5	3.8	3.7
	Total lignin	385	357	359	421	473	487	605

[a] Total range varying from Ci to Cj; Structural indexes: $(Ad/Al)_G$=G6/G4; $(Ad/Al)_S$=S6/S4; (Γ_G)=G6/(G14+G15); (Γs)=S6/(S14+S15).

Table 4 Composition[a] and yields (µg g^{-1}) of main TAHM products released from the field plots of Grandi project site

	Compounds	t0	Trad	0N	SSB	SSA	CMPB	CMPA
					1 year			
Lipids	Fatty acids	4465	4574	4481	4520	4583	4496	4523
	Microbial (%)	9.5	9	8	8.5	9	10	9
	Mid-chain hydroxy acids(C_{16}	351	344	352	365	359	372	362
	ω-Hydroxy acids (C_{16}÷C_{22})	288	274	285	310	304	324	335
	Alkanes(C_{25}÷C_{31})	95	85	87	92	102	87	93
	Alcohols C_{16}-C_{26})	75	70	68	79	82	72	75
	Phytosterols	92	85	87	95	103	110	114
	Total lipids	5366	5432	5360	5461	5533	5461	5502
Lignin	Guaiacyl	195	207	175	200	210	214	205
	$(Ad/Al)_G$[b]	3.2	3.3	3.4	3.5	3.1	3.3	3.4
	(Γ_G)[b]	3.4	4.0	3.7	3.4	3.2	3.3	3.4
	p-Hydroxyphenyl	181	154	163	199	212	214	226
	Syringyl	164	171	175	181	189	190	195
	$(Ad/Al)_S$[b]	4.0	3.9	3.8	3.9	3.8	4.1	3.9
	(Γ_S)[b]	3.2	3.1	3.3	3.1	3.0	3.3	2.9
	Total lignin	540	532	513	580	611	618	626
					2 year			
Lipids	Fatty acids		4276	4125	4612	4575	4563	4596
	Microbial (%)		7	7	8.5	10	10	9
	Mid-chain		298	335	374	383	390	405
	ω-Hydroxy acids		274	285	310	304	324	335
	Alkanes(C_{25}÷C_{31})		82	79	95	97	108	110
	Alcohols C_{16}-C_{26})		65	64	85	80	92	105
	Phytosterols		80	75	95	105	115	110
	Total lipids		5075	4963	5571	5544	5592	5661
L	Guaiacyl		192	185	208	225	227	232

$(Ad/Al)_G$[b]	3.4	3.6	3.2	3.1	3.2	3.1
(Γ_G)[b]	3.9	3.8	3.3	3.2	3.1	3.2
p-Hydroxyphenyl	152	172	206	232	245	256
Syringyl	170	154	189	196	194	205
$(Ad/Al)_S$[b]	3.9	3.8	3.9	3.8	4.1	3.9
(Γ_S)[b]	3.1	3.3	3.1	3.0	3.3	2.9
Total lignin	514	511	603	653	666	693

Table 5 Composition[a] and yields (μg g^{-1}) of main TAHM products released from the field plots of Castel Volturno project site

	Compounds	t0	Trad	0N	FeP	SSB	SSA	CMPB	CMPA
				1 year					
Lipids	Fatty acids C_{12}÷C_{28}	5475	5165	5422	5395	5560	5596	5585	5546
	Microbial (%)	11	10	9	10.5	10.5	9	11	10.5
	Mid-chain hydroxy	236	302	262	286	284	291	284	302
	ω-Hydroxy acids (C_{16}÷C_{22})	410	394	375	422	435	398	411	425
	Alkanes(C_{25}÷C_{31})	148	152	127	133	152	165	158	163
	Alcohols C_{16}-C_{26})	230	190	218	247	208	197	212	225
	Phytosterols	105	98	97	95	95	112	125	142
	Total lipids	6604	6301	6501	6578	6734	6759	6775	6803
Lignin	Guaiacyl	220	212	225	192	232	240	254	267
	$(Ad/Al)_G$[b]	4.1	3.9	3.7	3.9	3.8	4.1	4.0	3.9
	(Γ_G)[b]	3.6	3.7	4.0	3.8	3.5	3.6	3.5	3.7
	p-Hydroxyphenyl	222	234	193	215	219	224	235	247
	Syringyl	240	211	228	197	245	239	251	265
	$(Ad/Al)_S$[b]	4.0	4.0	3.8	3.9	3.8	4.0	3.9	3.9
	(Γ_S)[b]	3.4	3.3	3.6	3.5	3.3	3.4	3.3	32
	Total lignin	682	657	646	604	696	703	740	779
				2 year					
Lipids	Fatty acids		5370	5295	5412	5605	5622	5590	5624
	Microbial (%)		10	9.5	9	10	11	10.5	10.5
	Mid-chain		296	257	275	296	312	324	318
	ω-Hydroxy acids		378	362	402	429	412	395	420
	Alkanes(C_{25}÷C_{31})		155	158	162	171	175	149	165
	Alcohols C_{16}-C_{26})		196	202	195	212	224	231	238
	Phytosterols		87	85	92	96	118	125	146

	Total lipids	6482	6359	6538	6809	6863	6814	6911
	Guaiacyl	214	207	204	237	251	265	272
	$(Ad/Al)_G$[b]	3.9	3.9	3.7	3.6	3.8	3.7	3.7
	(Γ_G)[b]	3.7	3.9	3.8	3.5	3.4	3.4	3.5
Lignin	*p*-Hydroxyphenyl	228	214	195	224	237	242	265
	Syringyl	194	185	204	251	248	274	286
	$(Ad/Al)_S$[b]	4.0	3.8	3.9	3.8	4.0	3.9	3.9
	(Γ_S)[b]	3.5	3.6	3.5	3.3	3.3	3.3	3.2
	Total lignin	636	606	603	712	736	781	823

Table 6 Composition[a] and yields (µg g^{-1}) of main TAHM products released from the field plots of Prima Luce project site

	Compounds	t0	A	B	C	D
	1 year					
Lipids	Fatty acids C_{12}÷C_{28}	2468	2797	2820	3210	3228
	Microbial (%)	8	9.2	9.2	8.9	9.3
	Mid-chain hydroxy	118	96	95	196	244
	ω-Hydroxy acids (C_{16}÷C_{22})	210	158	142	285	297
	Alkanes(C_{25}÷C_{31})	84	102	98	172	194
	Alcohols C_{16}-	125	118	114	174	195
	Phytosterols	95	89	108	115	134
	Total lipids	3100	3360	3377	4152	4292
Lignin	Guaiacyl	185	198	175	227	218
	$(Ad/Al)_G$[b]	5.1	4.9	4.8	4.6	4.7
	(Γ_G)[b]	4.2	4.3	4.0	4.1	4.0
	p-Hydroxyphenyl	148	175	164	192	210
	Syringyl	140	177	157	235	248
	$(Ad/Al)_S$[b]	4.1	3.9	4.1	4.0	3.8
	(Γ_S)[b]	3.7	3.8	4.0	3.8	3.6
	Total lignin	473	550	496	654	676
	2 year					
Lipids	Fatty acids		2545	2369	3274	3357
	Microbial (%)		8.9	9.0	10.4	11.2
	Mid-chain		87	80	212	254
	ω-Hydroxy acids		144	117	291	322
	Alkanes(C_{25}÷C_{31})		93	97	173	202
	Alcohols C_{16}-		107	96	177	244

	Phytosterols	101	91	128	145
	Total lipids	3077	2850	4255	4524
Lignin	Guaiacyl	207	162	251	286
	$(Ad/Al)_G$[b]	4.4	5.0	4.4	4.3
	(Γ_G)[b]	4.1	4.1	3.9	3.9
	p-Hydroxyphenyl	182	148	226	258
	Syringyl	169	154	239	277
	$(Ad/Al)_S$[b]	3.9	4.0	3.8	3.8
	(Γ_S)[b]	4.0	4.1	3.7	3.6
	Total lignin	558	464	716	821

3.4 Humic acids

The 13C NMR spectra of humic acids obtained from the different project sites at initial time are shown in Figure 14 while the Table 7 indicate the relative C distribution among the main functional groups.

The signals found in the alkyl-C region (0–45 ppm) regions, revealed the large incorporation of alkyl chains pertaining to different components. The peaks at 16, 23 and 30 ppm may be derived mainly from CH3- and CH2- groups of various lipid compounds, such as waxes, polyesters, and phospholipids. In addition to the peaks between 0 and 30 ppm, distinct resonances were shown in the broad alkyl-C region around 30–45 ppm, which indicate the simultaneous presence of different alkyl chains from branched and ciclyc compounds (e.g. sterol) and peptide derivatives. The signal at 56 ppm may be associated with either the methoxyl substituent on the aromatic rings of guaiacyl and syringyl units in lignin structures. Besides the lignin compounds, the the 45–60 ppm chemical shift range may also include the C–N bonds in amino acid moieties.

The different resonances in the O-alkyl-C region (60–110 ppm) are currently assigned to monomeric units in oligo and polysaccharide chains of plant tissue. The intense signal around 72 ppm corresponds to the overlapping resonances of carbons 2, 3, and 5 in the pyranoside structure in cellulose and some hemicelluloses, whereas the signal at 104 ppm is assigned to the anomeric carbon 1 of the glucose unit in cellulose.

The shoulders localized around 65 and 88 ppm result from carbons 6 and 4 of monomeric units, respectively. Besides the signals usually assigned to cellulose, the spectra of different HAs revealed additional resonances around 94 98 ppm. These signals may be related, espectively, to the di-O-alkyl-C of monomeric units of simple carbohydrates and to the C1 of either hemicellulose or pectic polysaccharides chains contained in cell walls of plants, such as □-1,5 arabinan, □-1,4 galactan, and □-1,4 galacturonan.

In the aromatic/olefinic-C region (110–145 ppm), the different resonances around 120 and 130 ppm are related to unsubstituted and C-substituted aryl carbon pertaining to both lignin monomers and ring components of polyphenols. The evident resonances shown at 152 (sharp) and 158-ppm chemical shift range are usually assigned to carbons 3, 4, and 5 in the aromatic ring of lignin components, with carbon 3 and 5 being coupled to the corresponding

methoxyl substituents. The attenuated signal intensity shown by the specific O-aromatic region (145–160 ppm) in HAs, confirms the lower incorporation of O-substituted ring carbon derived from different lignin structures. Finally, all humic acids were characterized by the intense ignal in the carbonyl region (160–190 ppm) at 174 ppm suggesting the occurrence of intense oxidative processes .

The main properties of humic acids may be summarises by the calculation of dimensionless structural indexes. The hydrophobic index (HB) which is related to the overall biochemical stability of humic fractions, indicate that the HAs from Tetto Frati, Grandi and CastelVolturno has a large preservation of hydrophobic components, mainly attributable to aliphatic compounds, while the aromatic index (Ar) suggested the lower presence of plant derived lignin components in all humic materials. In this respect the comparison of signal intensity in the 45–60 ppm interval over that in the 140–160 ppm range, may be helpful for a more accurate assignment of methoxyl and phenolic resonances. This dimensionless index, hereby denoted as lignin ratio (LR), has been used to improve discrimination between signals from lignin units characteristic of other phenolic components or peptidic moieties. While a lower ratio around 1 is usually associated with the inclusion of tannin and polyphenol constituents to the global O-aromatic-C signals, the opposite prevalence of upper fractional part indicates the significant contribution of C–N bonds in the 45–60 ppm area. Therefore, the discrepancy between methoxyl-C and phenolic-C signals, summarized by the larger lignin ratio found in all humic extracts (Table 7), suggests the incorporation biolabile peptidic materials and a lesser preservation of lignin components in the stabilized organic fractions. Finally the larger amount of polysaccharides found in HA from Prima Luce (Fig. 3) revealed a steady maintenance of biolabile compounds showing a lower hydrophobic character (Table 7).

Table 7 Relative distribution (%) of signal area over the six main chemical shift regions (ppm) and structural indices of grouped C molecular types assessed by 13C CPMAS-NMR spectroscopy of the Humic acids extracted from initial soil samples (TF: Tetto Frati; GR. Grandi; CV. CastelVolturno; PL: Prima Luce)

Soil	Carboxyl	O-Aromatic	Aromatic	O-Alkyl	CH_3O/CN	Alkyl	Structural index [a]		
HAs	190-160	160-145	145-110	110-60	60-45	45-0	LR	HB	Ar
TF	10.9	4.4	13.3	29.3	15.8	26.3	3.6	1.08	17.7
GR	6.9	2.2	10.7	37.3	11.3	31.5	5.1	1.00	12.9
CV	12.4	4.6	13.2	23.3	18.0	28.5	3.9	1.24	17.7
PL	11.3	2.8	12.7	42.1	12.5	18.7	4.55	0.68	15.4

LR Lignin ratio = (60-45)/(145-110)

HB Hydrophobic index= Σ (45-0)+(60-45)/2+(110-160)/Σ (60-45)2+(60-110)+(160-190)

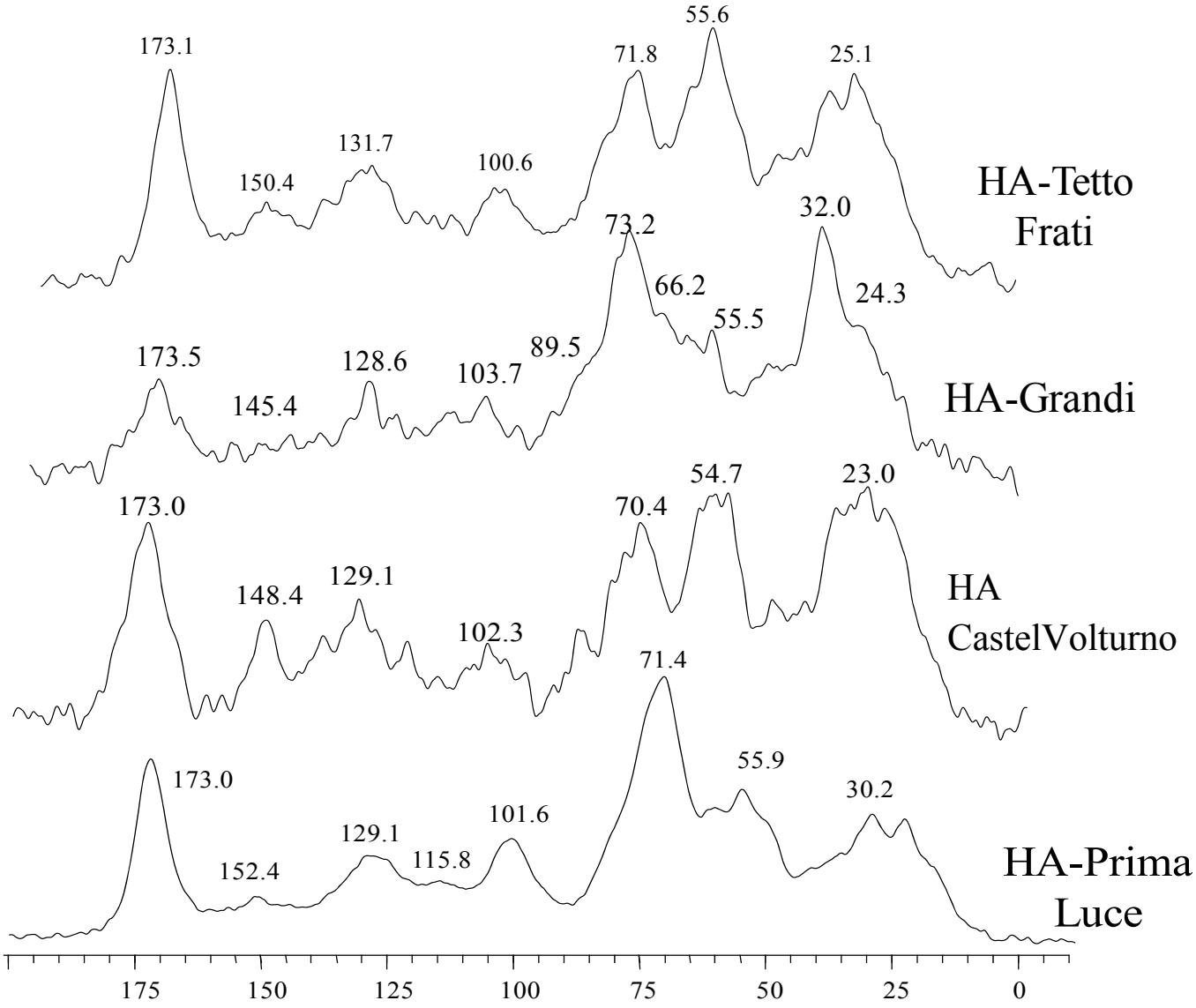

Figure 14 13C CPMAS NMR spectra of control soils at initial experimental time

3.5 Biological analyses

3.5.1 PLFA: Project sites Tetto Frati, Grandi, Castel Volturno

The Table 7 report the main PLFA associated with the different microbial communities

Table 7. Main PLFA biomarkers associated with different microbial groups

Microbial	Fatty acid
GRAM+ bacteria	a15:0
GRAM+ bacteria	15:00
GRAM+ bacteria	i16:0
GRAM+ bacteria	a16:0
GRAM- bacteria/FUNGI	16:1w7c
ARBUSCULAR MYCORRHYZA	16:1w5c
GRAM- bacteria	cy16:0
ACTINOMYCES	10Me16:0
GRAM+ bacteria	i17:0
GRAM+ bacteria	a17:0
GRAM- bacteria	cy 17:0
GRAM+ bacteria	17:00
FUNGI	18:2 w 6,9
FUNGI	18:1w9c

The PLFA analyses revealed differences among the control soils of each project site, with a larger yields in the field plots of Grandi in respect to the University farms of Torino and Napoli. This finding may be related to the different soil managements currently applied in the different sites, with the organic farming usually applied in the commercial farms promoting a stable high biological activity as compared to the conventional cropping systems, based on chemical fertilizer adopted at Tetto Frati and Castel Volturno

The released PLFA showed significant increase of total biomass in all field plots added with different organic materials. A large increase was found for the project sites of Tetto Frati and Grandi in the soil treatments with fresh solid digestate. This result may be related to the larger presence of bioavailable components (e.g. peptides, carbohydrates) in fresh organic residues in respect to stable humified composts, which can easily support the development of microbial communities. Although the soil addition with decomposable materials may have negative effect of the overall SOC stability (priming effect) the results of SOC analyses on SSB and SSA treatments did not show any evidence of detrimental response on SOC thereby suggesting the mutual beneficial effect on the different SOC pools. Moreover the soil treatments with organic amendments promoted also an increase of the NLFA associated with the arbuscular mycorrhyza fungi that represent important symbiotic organisms for the mobilisation of the available fraction of soil phosphorus.

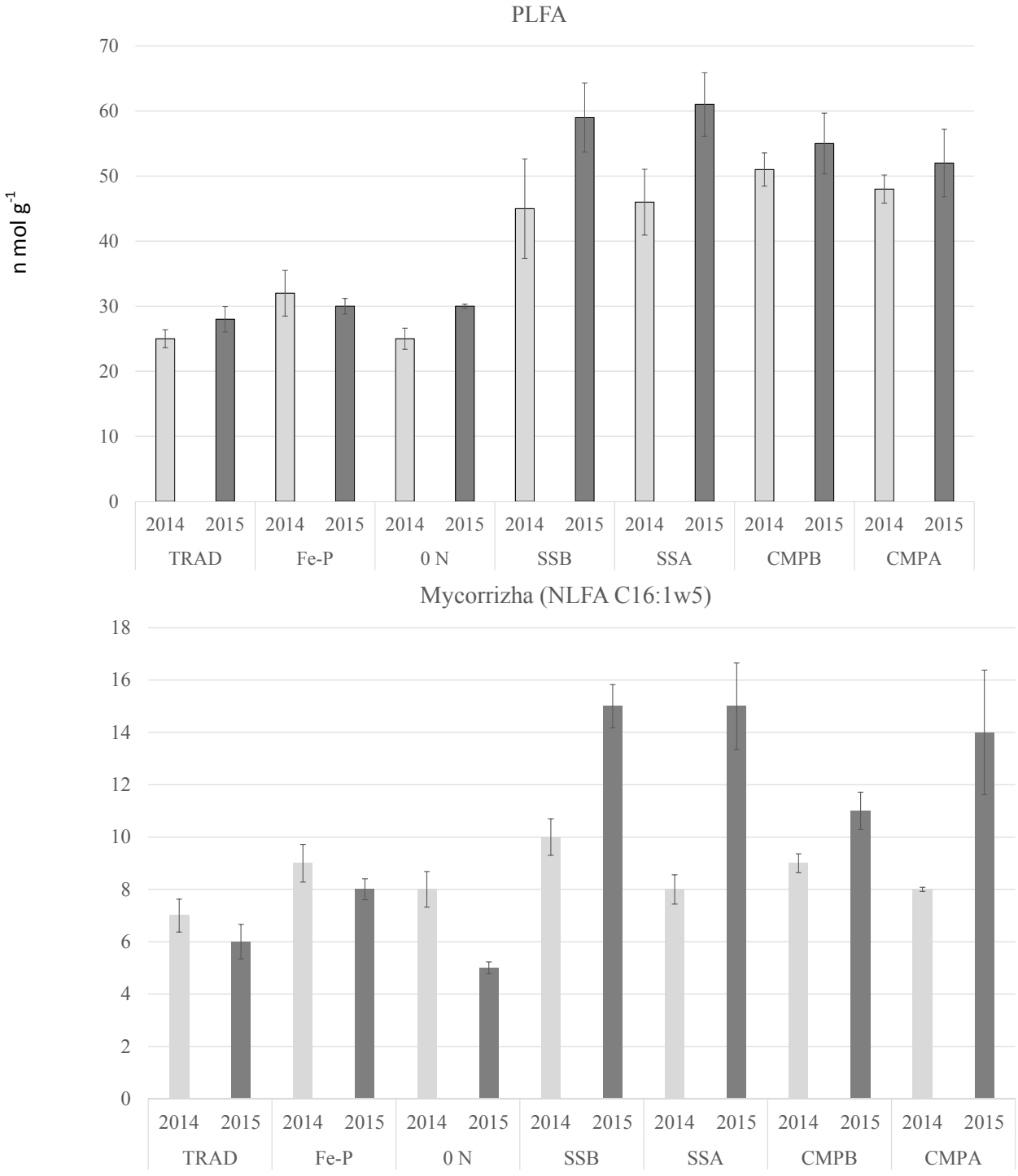

Figure 14 Total PLFA and AMF-NLFA released by soil treatments of Tetto Frati

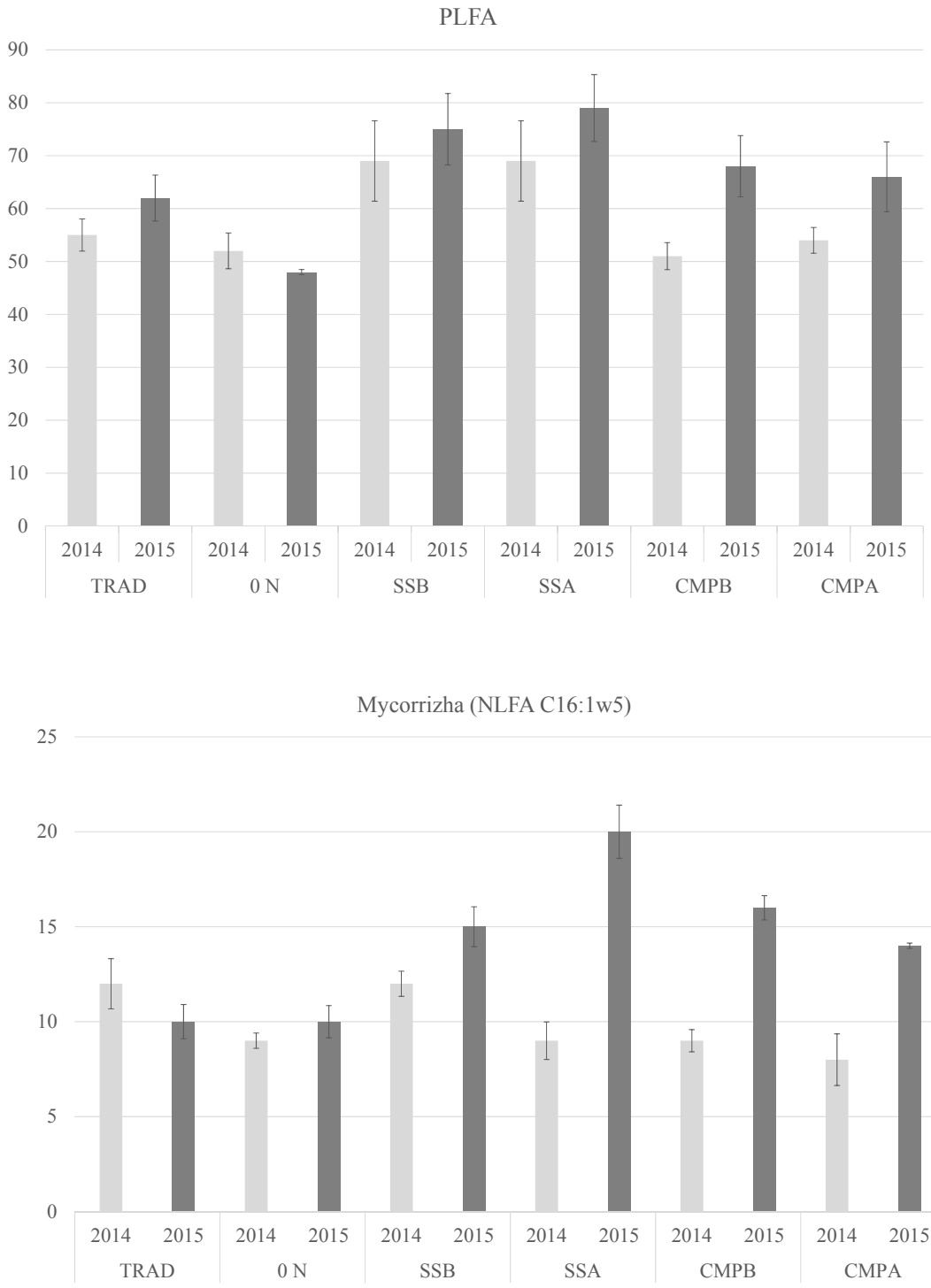

Figure 15 Total PLFA and AMF-NLFA released by soil treatments of Grandi

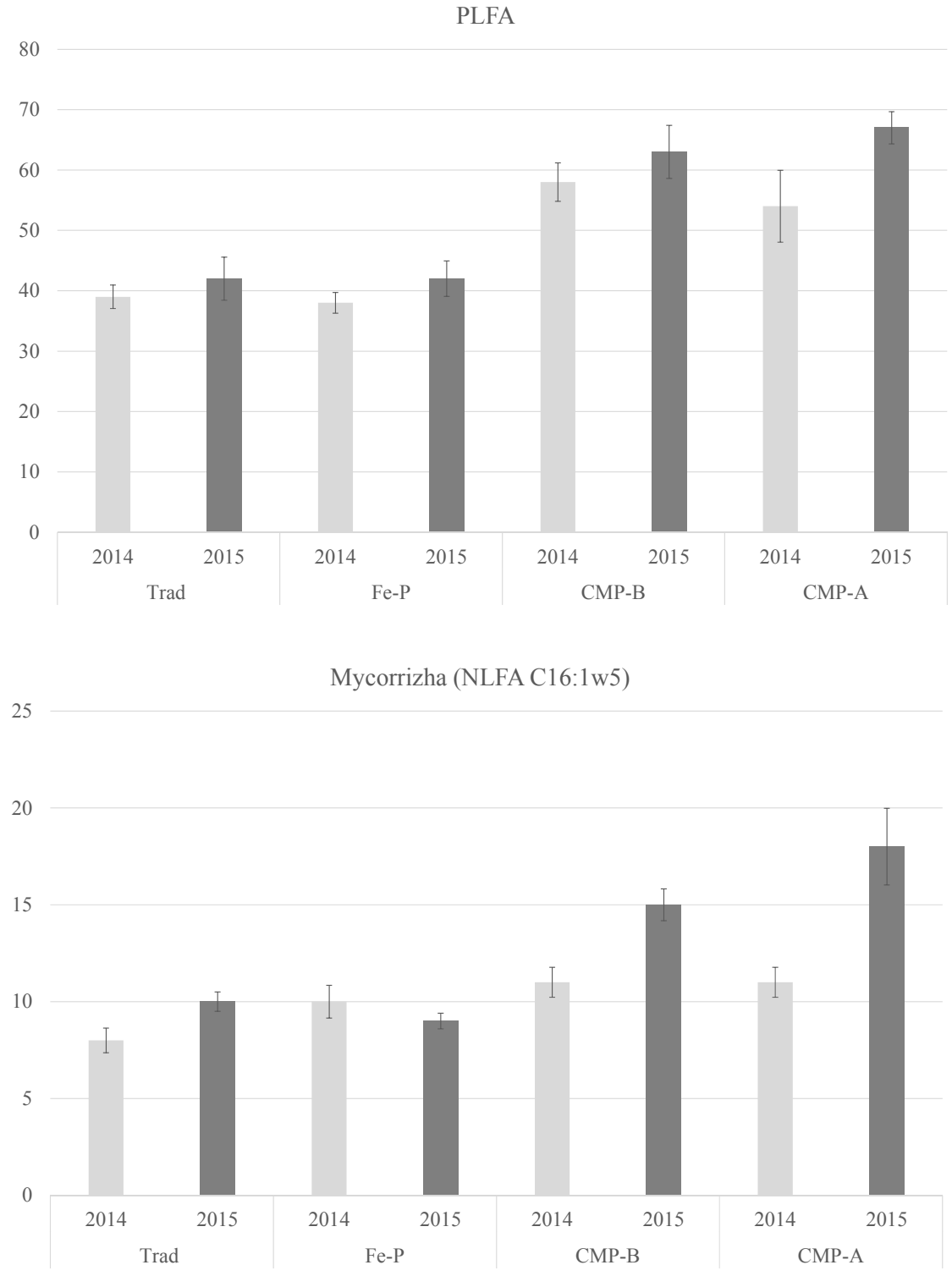

Figure 16 Total PLFA and AMF-NLFA released by soil treatments of Castel Volturno

3.4.2 Project site Prima Luce

- Enzimatic activity

On September 2015, after one year from the first amendment, soil samples for monitoring of biological fertility were collected and characterized for the main biological and biochemical soil properties. In particular, will be monitored generic enzymatic activities involved in the degradation of organic matter, as dehydrogenase and hydrolase, but also specific enzymes involved in carbon cycle (β-glucosidase, β-galactosidase, glucosaminidase and invertase), in phosphorus and sulphur cycles (phosphomonoestarase and arylsulphatase) or in nitrogen cycle (urease, nitrate reductase and protease). Moreover, to evaluate the effects of compost on soil microbial community, carbon and nitrogen biomass and microbial respiration will be monitored. Influence of the compost on functional biodiversity and catabolic profiling of soil microorganisms, were studied by Biolog Ecoplate, that allows measurement of catabolic activity against 31 different carbon substrates. Finally, soil microbial community will be analyzed by API-ZYM strips too.

Most of the analysis are still ongoing, but the firsts characterization by catabolic profiling are completed and available. The effect of soil organic amendment on the utilization of different carbon and nitrogen sources by soil microbial community, determined by BIOLOG Ecoplates□, was evaluated by analysis of variance (one-way ANOVA). Results showed that the catabolic activity of soil microorganisms was significantly affected by organic treatment only for 4 of the 31 analyzed substrates: D-Xylose, L-Phenylalanine, L-Threonine and D-Cellobiose (Table 8), that are both easily degradable substrates, such as amino acids, and more complex carbon compound as carbohydrates. Moreover, Biolog catabolic profile was used to determine the AWCD and the Shannon's biodiversity index (Fig 16). The AWCD showed differences between the soil treatments after 48 h of incubation, with the higher values in the plots under 20 Mg ha-1 of compost (Fig. 17). Although the differences of the Shannon's biodiversity index values of the soils under different organic amendment were not very strongly, also in this case plots under the highest dose of compost (20 + 20 Mg ha-1) showed the highest value (Fig. 16 B). After one year and two amendments, the BIOLOG method did not revealed deep changes in soil microbial community catabolic characteristics, resulting in a different utilization of carbon sources. Only the catabolic activity of the plots under the highest dose of compost, was affected by organic amendments and able to metabolize carbon substrates in different way. The low rate of used compost and the short period of observation, could be taken into account to explain this results. Anyway, the other soil biological and biochemical characterization, useful to understand this phenomena, are still ongoing.

- Ergosterol content in soil.

Preliminary results showed average values of 0.88 µg of ergosterol per gram of soil (d.w.) in non fertilized (control) plots and 2.51 µg g-1 d.w. in the plots amended with 20 + 20 t/ha of compost. This indicates that 20 + 20 t/ha of compost stimulates the growth of the fungal biomass, whose amount were almost triple than control after two amendments.

However, the peculiar texture of the studied soil made difficult the separation of cyclohexane from the hydrophilic phase, since most soil debris placed at the interface during the centrifugation step. This problem was firstly minimized increasing the amount of cyclohexane. However, further tests are necessary in order to optimize the extraction procedure to this kind of soil, before reaching a standardized method applicable to all the samples to obtain definitive and complete results.

Table 8. ANOVA one way for all carbon substrates utilized by microorganisms in Biolog Ecoplates (n = 12 samples) and their numbering. Type of treatment (3 d.f.) was the independent variable

			Type of treatment	
Type	Number	Substrate	F	P value
Carbohydrates	A2	□-Methyl-D Glucoside	2.9155	0.1005
Carbohydrates	A3	D-Galactonic Acid □-Lactone	2.4808	0.1353
Amino acids	A4	L-Arginine	0.5122	0.6851
Caboxylic acid	B1	Pyruvic Acid Methyl Ester	0.7781	0.5384
Carbohydrates	B2	D-Xylose	5.4867	0.0242*
Caboxylic acid	B3	D-Galacturonic Acid	2.8363	0.1060
Amino acids	B4	L-Asparagine	0.4846	0.7022
Polymers	C1	Tween 40	0.4773	0.7069
Carbohydrates	C2	i-Erythritol	0.7293	0.5628
Phenols	C3	2-Hidroxy Benzoic Acid	1.0279	0.4303
Amino acids	C4	L-Phenylalanine	8.0414	0.0085*
Polymers	D1	Tween 80	0.3471	0.7924
Carbohydrates	D2	D-Mannitol	1.4929	0.2886
Phenols	D3	4-Hydroxy Benzoic Acid	1.1825	0.3757
Amino acids	D4	L-Serine	0.1507	0.9263
Polymers	E1	□-Cyclodextrine	1.7225	0.2393
Carbohydrates	E2	N-Acetil-Dglucosamine	0.3132	0.8156
Caboxylic acid	E3	g-Hydroxybutyric Acid	1.1593	0.3833
Amino acids	E4	L-Threonine	5.7462	0.0215*
Polymers	F1	Glycogen	1.8859	0.2104
Caboxylic acid	F2	D-Glucosaminic Acid	0.0636	0.9776
Caboxylic acid	F3	Itaconic Acid	0.7766	0.5392
Amino acids	F4	Glycil-L-Glutamic Acid	1.8515	0.2161
Carbohydrates	G1	D-Cellobiose	8.1247	0.0082*
Carbohydrates	G2	Glucose-1-Phosphate	0.7896	0.5329
Caboxylic acid	G3	□-Ketobutyric Acid	2.5685	0.1272
Amines/amides	G4	Phenyletyl-amine	1.0365	0.4270
Carbohydrates	H1	□-D-Lactose	0.6386	0.6111
Carbohydrates	H2	D,L-□-Glycerol Phosphate	2.0060	0.1244
Caboxylic acid	H3	D-Malic Acid	0.6072	0.6287
Amines/amides	H4	Putrescine	0.6340	0.6137

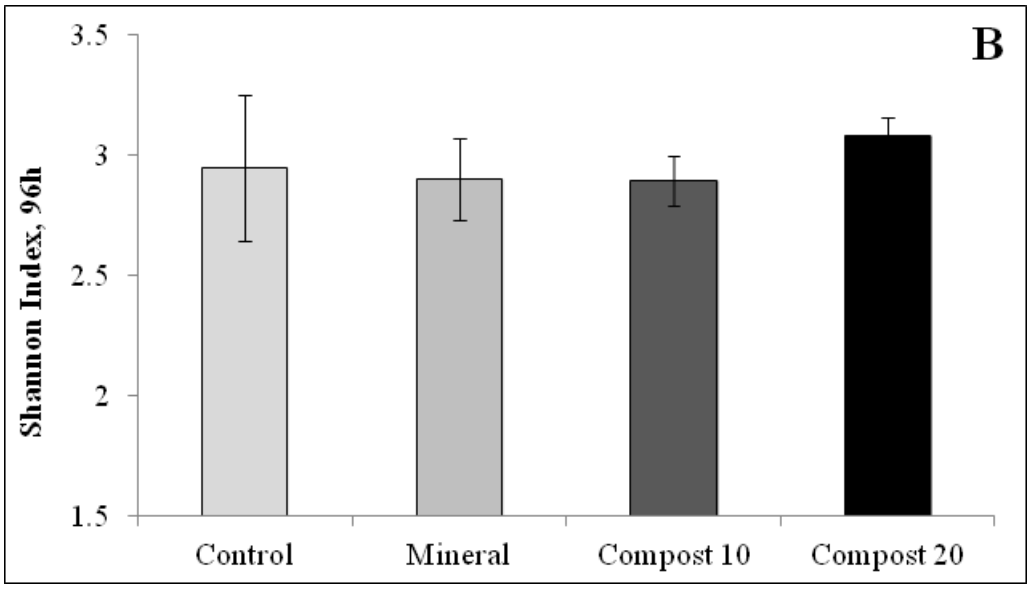

Figure 17. Average well-color development (AWCD, panel A) and Shannon–Weaver index (panel B) of metabolized substrates in BIOLOG EcoPlate™ by the microbial communities of soil under different organic amendment. Control: control soil no treated; Mineral: organic-mineral amendment, 100 kg N ha^{-1}; Compost 10 and 20: compost amendment, 10 and 20 Mg ha^{-1}, respectively.

3.6 Project site Mellone: Soil analysis at starting time (T0): C and total N contents, C/N ratio

Soils were characterized before compost amendments in order to assess changes in soil chemical parameters along time. Particularly, total nitrogen (Kjeldhal method) and organic carbon contents, and C to N ratio were determined.
An analysis procedure was standardized in order to identify representative soil sampling points. In particular, EMI acquisitions were saved, corrected, exported in GIS and spatialized in raster format. Then, soil sampling points (n=12 per each species orchard) were identified using the ESAP software. These sampling points represented maximum different areas within the orchards which were, for this reason, indicative of the extreme variations of soil characteristics. A detailed description of this analysis procedure can be found in the Progress report - Annex Report Action B.3.

Table 9 - Means and standard deviation of Carbon and total N content and C/N ratio of soil sampled from the kiwi orchard. Number sequence (from 1 to 12) represent sampling points identified by means of the ESAP software starting from EMI maps

Sample	% dry soil		
	N	C	C/N
kiwi 1	0.18	1.85	10.23
kiwi 2	0.18	1.74	9.79
kiwi 3	0.12	1.66	13.41
kiwi 4	0.16	1.59	10.21
kiwi 5	0.12	1.76	14.15
kiwi 6	0.10	1.81	17.49
kiwi 7	0.14	1.76	12.55
kiwi 8	0.17	1.70	10.05
kiwi 9	0.14	1.78	13.11
kiwi 10	0.14	1.81	12.54
kiwi 11	0.14	1.90	14.09
kiwi 12	0.11	1.95	16.95
Mean	**0.14**	**1.78**	**12.88**
St. dev.	**0.0247**	**0.099**	**2.58**
RSD%	**17.40**	**5.55**	**20.03**

Table 10 - Means and standard deviation of Carbon and total N content and C/N ratio of soil sampled from the peach orchard. Number sequence (from 1 to 12) represent sampling points identified by means of the ESAP software starting from EMI maps

Sample	% dry soil		
	N	C	C/N
Peach 1	0.14	1.97	14.14
Peach 2	0.18	1.97	11.06
Peach 3	0.16	1.84	11.57
Peach 4	0.13	1.57	11.66
Peach 5	0.13	1.52	11.85
Peach 6	0.11	1.57	14.67
Peach 7	0.11	1.54	14.64
Peach 8	0.13	1.55	11.94
Peach 9	0.13	1.68	13.38
Peach 10	0.12	1.70	13.63
Peach 11	0.10	1.63	16.91
Peach 12	0.11	1.61	14.57

As expected, sustainable soil management (cover crops and pruning material recycle within the fruit orchard) applied for more than 10 years allowed to increase N and C contents in both fruit orchards studied (N: 0,142% and 0,128% in kiwi orchard and peach one, respectively; C: 1,54% e 1,65% in kiwi orchard and peach one, respectively).

The studied parameters were more variable in the peach orchard then in the kiwi one. Maps obtained by means of GIS software showing the spatial distribution of the above mentioned parameters are reported in figures 18 (kiwi orchard) and 19 (peach orchard).

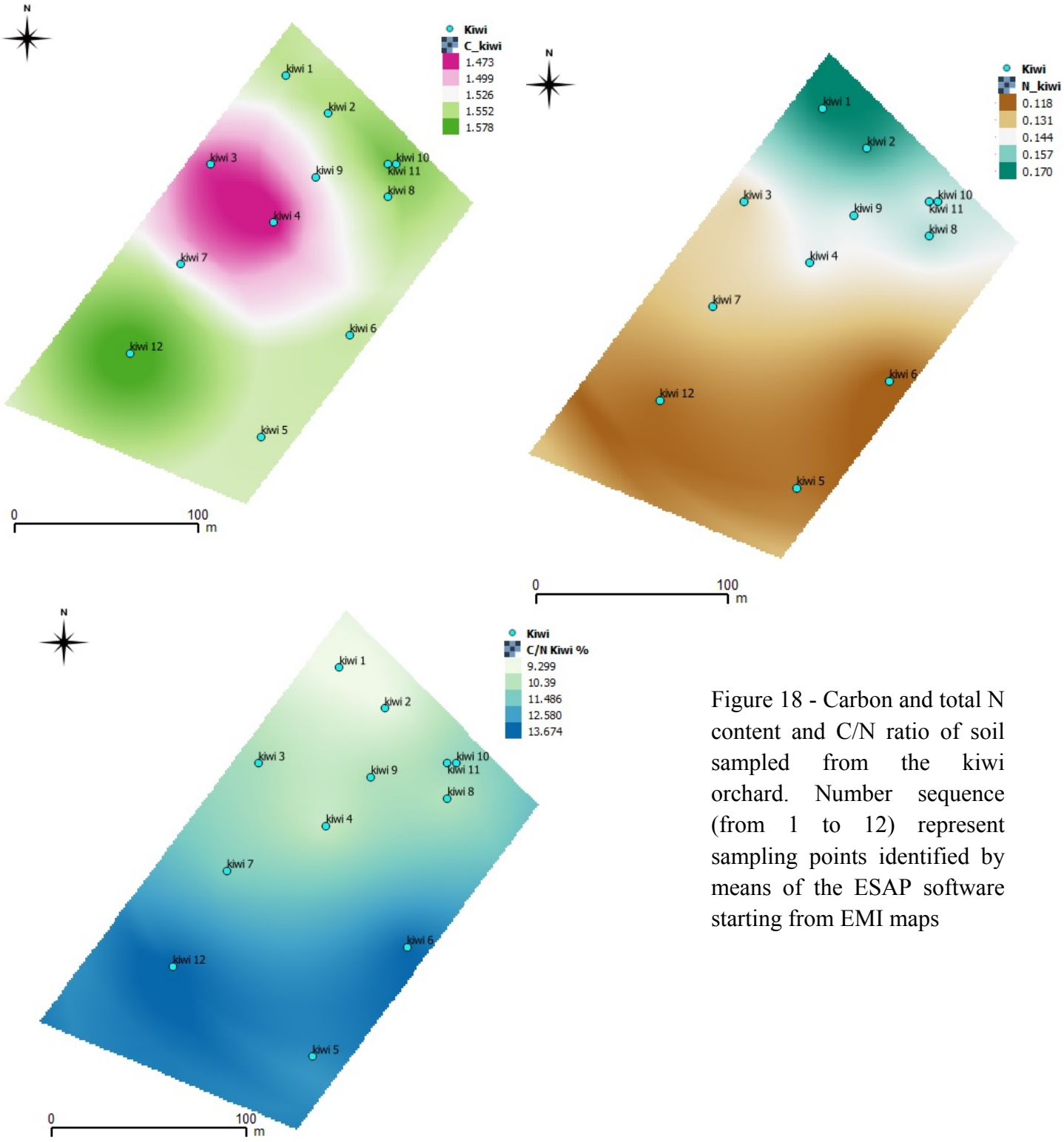

Figure 18 - Carbon and total N content and C/N ratio of soil sampled from the kiwi orchard. Number sequence (from 1 to 12) represent sampling points identified by means of the ESAP software starting from EMI maps

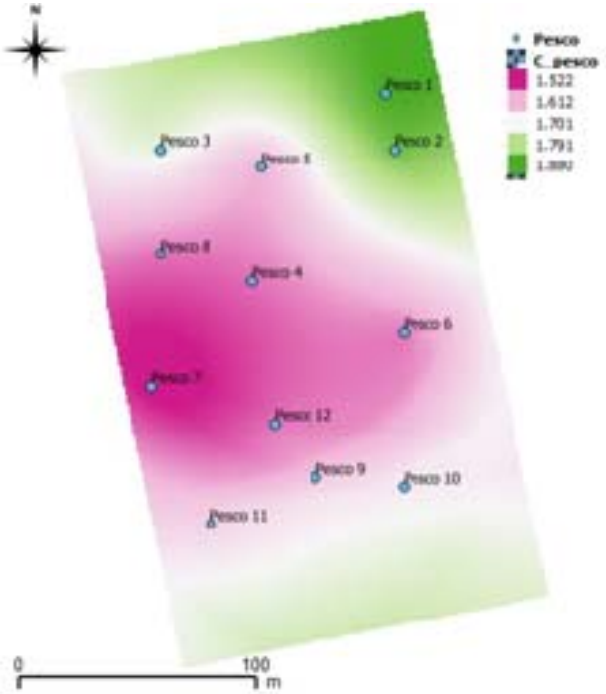

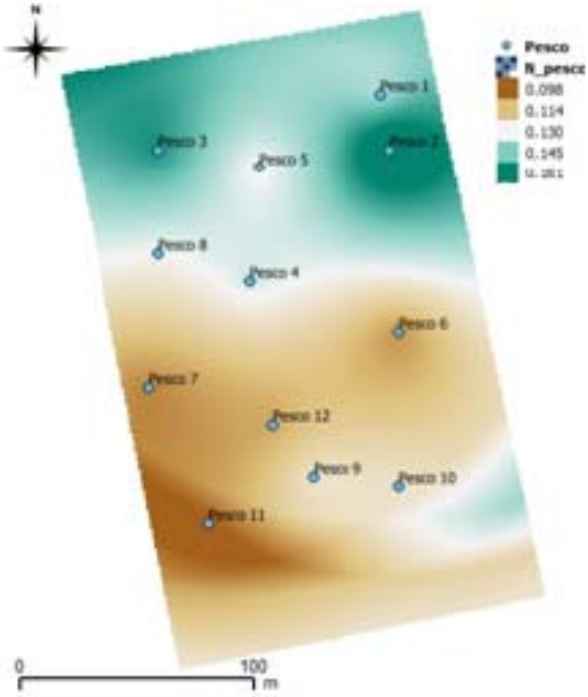

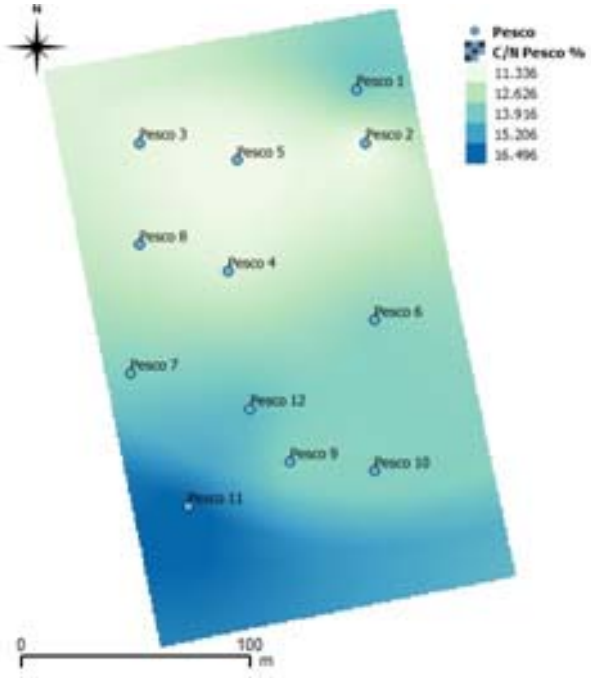

Figure 19 - Carbon and total N content and C/N ratio of soil sampled from the peach orchard. Number sequence (from 1 to 12) represent sampling points identified by means of the ESAP software starting from EMI maps